# Mesoporous Silica Nanoparticles as Carriers for Biomolecules in Cancer Therapy

Küçüktürkmen, Berrin; Rosenholm, Jessica M.

*Published in:*
Bio-Nanomedicine for Cancer Therapy

*DOI:*
10.1007/978-3-030-58174-9_5

Published: 02/02/2021

*Document Version*
Accepted author manuscript

*Document License*
Publisher rights policy

# MESOPOROUS SILICA NANOPARTICLES AS CARRIERS FOR BIOMOLECULES IN CANCER THERAPY

**Berrin Küçüktürkmen[1,2] & Jessica M. Rosenholm[1]**

*[1]Pharmaceutical Sciences Laboratory, Faculty of Science and Engineering, Åbo Akademi University, Finland*
*[2]Department of Pharmaceutical Technology, Faculty of Pharmacy, Ankara University, Turkey*

**Abstract**

Mesoporous silica nanoparticles (MSNs) offer many advantageous properties for applications in the field of nanobiotechnology. Loading of small molecules into MSNs is straightforward and widely applied, but with the upswing of both research and commercial interest in biological drugs in recent years, also biomacromolecules have been loaded into MSNs. MSNs possess many critical properties making them a promising and versatile carrier for biomacromolecular delivery. In this chapter, we review the effects of the various structural parameters of MSNs on the effective loading of biomacromolecular therapeutics, with focus on maintaining stability and drug delivery performance. We also emphasize recent studies involving the use of MSNs in the delivery of biomacromolecular drugs, especially for cancer treatment.

## 1. Introduction

Amorphous silica is classified as GRAS (generally recognized as safe) by the FDA, and has in nanoparticulate form recently received FDA approval for stage I human clinical trials of fluorescence-based cancer imaging (1-3). MSNs offer many advantageous properties, useful for applications in the field of nanobiotechnology; e.g. as controllable particle size and pore size, robust morphology, large surface area, ease of inner/outer surface modification, high cargo loading capacity and efficient cargo transfer efficiency, low cytotoxicity, excellent biocompatibility and biodegradability properties, and cost-effective production (4-6). For all these reasons, MSNs with small particle size but large pore size have great potential to effectively overcome multiple drug resistance (MDR) by delivering biomacromolecules (peptides, proteins, or nucleic acids) into drug-resistant cancer cells (6). Numerous MSN nanocarriers smaller than 200 nm in diameter can penetrate tumor tissues due to the enhanced permeability and retention (EPR) effect. However, as for any prospective nanopharmaceuticals, there are some obstacles in the application of MSNs for tumor treatment such as tumor targeting deficiency and strong affinity of MSNs to blood proteins. In order to increase the active targeting effect, zero premature drug release and release at the targeted cancer sites should be considered based on differences between intratumoral and normal cell microenvironments. Therefore, surface functionalization is necessary to equip them with the ability to target tumors and increase the stability of blood circulation *in vivo* (7, 8). In addition, the biodegradability of MSNs should be optimized to prevent unwanted accumulation in the body that may cause acute or subacute inflammation or long-term biosecurity risks (9).

Biological medicines (biologicals, biologics) are one of the most promising areas for the implementation of MSNs as drug / gene delivery carriers. It has previously been well documented that proteins maintain increased activity and stability when loaded into the pores of MSNs, since the solid inorganic framework can efficiently protect proteins from denaturation (10). To date, MSNs with different morphologies have been synthesized: hollow mesoporous nanocapsules, branched mesoporous nanoparticles, yolk-shell mesoporous structures and so forth. Particularly in the diagnosis/imaging and treatment of cancer, functional nanoparticles such as magnetite, gold, quantum dots and anticancer drugs incorporated as core materials in core-shell designs, doped into the mesoporous silica matrix or loaded into the pore channels, have shown great application potential in the field of biological medicine (11).

## 2. Synthesis of MSNs

MSNs are commonly synthesized using cetyltrimethylammonium bromide (CTAB) micelle-templated sol-gel technique. The main disadvantage of this method is that the pores of the MSNs produced are small and the particle size homogeneity is insufficient. In the CTAB micelle-templated sol-gel technique, tetraethyl orthosilicate (TEOS) is first hydrolyzed and produces negatively charged silicate oligomers that approach and interact with positively charged CTAB micelles by electrostatic interaction. The condensation of the silicate oligomers then leads to the collection of silica nanoparticles and micelles (self-assembly). Aggregation ends when the surface net negative charge is high enough to prevent further growth, which results in the formation of MSNs with specific morphologies (4).

Mesoporous silica materials such as MCM-41, SBA-15, MCF and FMS have been successfully used as supports for the immobilization of biomolecules (see Figure 1). However, the 2D pore architecture and relatively small pore volume of these materials limit the diffusion and transport of biomolecules. To overcome this problem, researchers have used mesoporous silicas with 3D cubic pore channels such as FDU-12, KIT-5 and KIT-6. These materials have more accessible pores due to the interconnected cage-type pore structures and thus, can effectively increase the adsorption capacity. The silica framework is negatively charged at neutral pH, making it inherently suitable for loading of biomolecules with an isoelectrical point (IEP/pI) over 7 (i.e. positive charge at neutral pH). However, most therapeutically active proteins and all nucleic acids are negatively charged at neutral pH, creating electrostatic repulsion with the carrier material at suitable loading conditions. Thus, the mesoporous silica surface can be functionalized with different organic groups such as thiol, phenyl, vinyl, amine and carboxylic acid to increase the application potential in different fields and enhance the affinity to the full range of biomacromolecules (12).

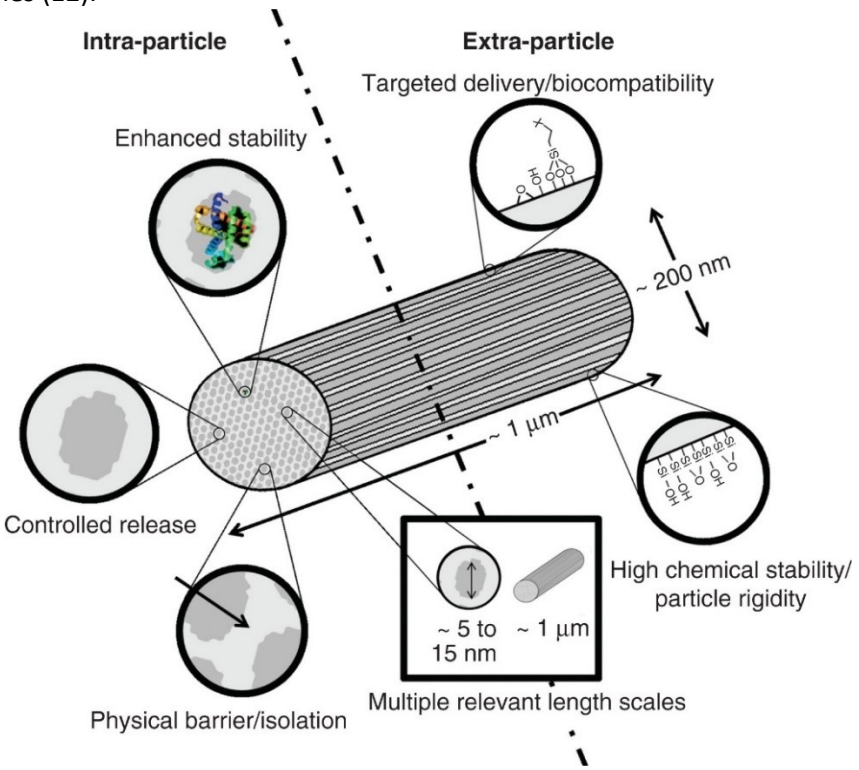


**Figure 1**. Design aspects of mesoporous silica SBA-15, highlighting their possible application to address intra- and extra-particle challenges that are especially relevant in biomacromolecular delivery. Reproduced from J. Siefker et al. (13)

The surfactant-micelle-templating method is a widely used method also in the synthesis of MSNs with large pores, suitable for the encapsulation of macromolecules. In this method, the micelle size is adjusted by adding a swelling agent as well as changing the surfactant. However, the swelling agent tends to induce irregularity or heterogeneity in the resulting structures. It has been reported that when the swelling agents have moderate solubility in the surfactant micelles, well-defined micelle-templated structures with substantially enlarged pores can occur. For example, for Pluronics having a high hydrophobic block fraction, such as Pluronic P123, it is advantageous to use low or moderately soluble swelling agents therein to prevent over-swelling. On the other hand, Pluronics having a low hydrophobic block fraction, such as Pluronic F127, work well with stronger swelling agents and allows the synthesis of silicas and organosilicas with large spherical mesopores. The resulting large-pore silicas and organosilicas with spherical and cylindrical mesopores have thick walls and thermal treatments can maintain the original pore shape and symmetry to ensure the formation of closed porous silicas. A variety of compounds were shown to act as micelle expanders, including benzene and its alkyl-substituted derivatives (most notably, 1,3,5-trimethylbenzene (TMB), 1,3,5-triethylbenzene (TEB), and 1,3,5-triisopropylbenzene (TIPB)), linear hydrocarbons (hexane), cyclic hydrocarbons (cyclohexane), and long-chain amines (14).

### 2.1. Large Pore MSNs for Macromolecular Drugs

Although delivery of small molecules has been shown to be quite successful in numerous examples, even in clinical studies (15), encapsulation of large therapeutic biomolecules such as proteins or DNA is limited due to the small pore size of conventional MSNs ranging from 2 to 5 nm. Compared to traditional MSNs, large-pore MSNs (LPMSNs) with pore sizes reaching the upper limit of mesopores (6-50 nm) have desirable properties for encapsulation of large molecules such as nucleic acids, enzymes or peptides into their porous structure (16).

Recently, two main approaches have been developed to produce LPMSNs. The first one is a solvent evaporation-induced self-assembly approach using high molecular weight block copolymers as the pore template. In this method, it is essential to use an unusual and costly fluorocarbon surfactant to control particle growth. Although the products obtained in this case have ultra-large pore channels, they have generally had irregular particle morphologies and micrometer particle sizes, which are unsuitable for intracellular delivery applications. The second approach is the use of pore expansion agents such as TMB during the synthesis of MSNs. Unfortunately, the pore expansion agent used causes irregularity and even complete destruction of the resulting mesostructure. Furthermore, the nanoparticles formed generally have a particle size of greater than 250 nm, which is expected to result in rapid removal of the particles from the circulation and a significant reduction in cellular uptake efficiency (11, 16, 17). Recently, large pore mesoporous organosilica NPs (18), large pore hollow dendritic MSNs (19, 20), extra-large pore MSNs (XL-MSNs) (21) have been synthesized for the delivery of macromolecules with different structures. Despite extensive efforts to develop large-pore MSNs, there are still some critical limitations to their use in macromolecular drug delivery. Therefore, new approaches and synthetic pathways are already needed for the synthesis of MSNs with accessible large pores (>10 nm), small particle sizes (<200 nm) and well-regulated mesostructures.

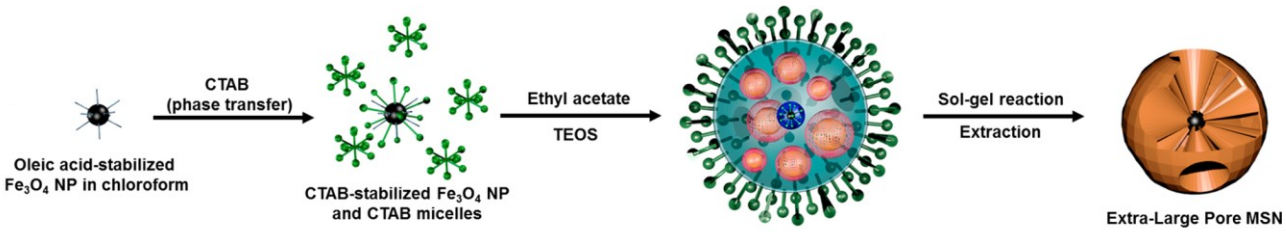


**Figure 2.** Synthesis of XL-MSNs. Reproduced from Kwon et.al. (21)

Although recent studies on the preparation of large-pore MSNs using co-solvents, block-copolymers and swelling agents, the preparation of discrete LPMSNs with high colloidal stability remains a challenge for efficient *in vivo* delivery (21, 22). Kwon et.al. (2017) synthesized uniform XL-MSNs in sizes 100, 150 and 180 nm with large pores over 30 nm for MSN-based *in vivo* cytokine delivery for immune cell modulation. To prepare large mesopores by providing high colloidal stability, CTAB-stabilized iron oxide nanoparticles were used in the sol-gel reaction as well as a high proportion of ethyl acetate as a pore expansion agent (Figure 2). To investigate the effect of iron oxide nanoparticles, the MSNs were prepared without CTAB-stabilized iron oxide nanoparticles but with the addition of a high proportion of ethyl acetate. Although the formed MSNs have large pores, the particle morphology was observed to be irregular and the pore size distribution was not as distinct as XL-MSNs. This suggests that CTAB-stabilized iron oxide nanoparticles serve as the initiator of the silica sol-gel reaction to form uniform XL-MSNs. The prepared XL-MSNs have also been shown to be applicable for loading proteins of different sizes. The loading of ovalbumin (OVA), bovine serum albumin (BSA), and glucose oxidase in 180 nm XL-MSNs was found to be 3.5-, 9.3-, and 6.2-fold higher than that in conventional MSNs, respectively. In this study, bioactive IL-4 was successfully delivered to macrophages by phagocyte targeting and induced M2 macrophage polarization in vivo (21). Similar to this study, Cha et.al. (2018) synthesized XL-MSNs as a cancer vaccine through the delivery of OVA and CpG oligonucleotide. To prepare large mesopores while maintaining high colloidal stability in MSNs, they employed a large amount of ethyl acetate, an organic additive, as a pore expansion agent in the presence of CTAB-stabilized iron oxide nanoparticles and seed material in a silica sol−gel reaction. Pore size distribution showed that XL-MSNs had bimodal pores that peaked at 3.2 nm and around 25 nm in the range between 10 and 30 nm. Amine-modified XL-MSNs resulted in significantly higher loading of OVA and CpG oligonucleotide compared with conventional small-pore MSNs (22). In another study, Zhang et.al. (2011) synthesized magnetic MSNs using TEOS as the source of silica, cationic surfactant CTAB as template, and TIPB/ decane as pore swelling agent. While adding the amount of TIPB in a limited range increased pore size, further use of TIPB resulted in severe particle coalescence and irregular pore structure. On the other hand, effective pore expansion of the magnetic MSNs was achieved by adding a suitable amount of decane together with a limited amount of TIPB. The obtained magnetic MSNs yielded smaller particle sizes (about 40–70 nm in diameter), tunable pore sizes (3.8–6.1 nm), high surface areas and large pore volumes. In addition, a strong correlation was found between increasing pore size and drug loading and the maximum loading capacity of the salmon sperm DNA (375 mg/g) was obtained using a magnetic MSN sample with the largest pore size of 6.1 nm (23).

Recently, large pore dendritic MSNs with hollow cavities have been synthesized and demonstrated superior advantages over dendritic MSNs in protein loading and controlled release. Hollow cavity reduces pore density and increases pore volume and hence, loading efficiency (19). Dendritic MSNs with opening pore channels are promising carriers with large pore sizes (34-45 nm). They have a high accessible internal surface area for the delivery of large molecule therapeutic agents such as plasmid DNA (*p*DNA) and proteins into cells. Meka et al. (2016) produced amine-functionalized hollow dendritic MSNs with a core

cavity of 170 nm and a mesopore in the shell of 20.7 nm. IgG (658 μg/mg) and β-galactosidase (391 μg/ mg) were found to be loaded in high amounts into the MSNs. Cellular uptake of β-galactosidase by hamster ovary cells (CHO-K1) increased, and MSNs maintained its catalytic properties within the cell. In this study, it was stated that using both TEOS and (3-aminopropyl) triethoxysilane (APTES) as the silica source is the most important parameter for the formation of large porous dendritic organic MSNs with hollow cavity. In the absence of APTES, hollow structures were not formed, and in the absence of TEOS, aggregates of amorphous silica molecules were obtained (19). Hong et al. (2018) synthesized polydopamine and chelated $Ti^{4+}$ modified dendritic MSNs with a central-radial pore structure for phosphopeptide enrichment. The synthesized MSN formulation had a particle size of approximately 150 nm and a wide pore size of 18.8 nm. This formulation was compared with conventional MSN and commercial $TiO_2$ in terms of phosphopeptide enrichment in various biological samples (including standard phosphoprotein, nonfat milk, human serum, and HeLa cell extracts). Low phosphopeptide detection limit of 0.2 fmol/ μL and an extremely high specificity (> 95%) of phosphopeptides identified from HeLa cell extracts were obtained (24).

MSNs are also of great importance for enzyme immobilization. Once the enzymes have been loaded into MSNs, their enzymatic activity is maintained over a wide pH range and even after exposure to enzyme degrading agents such as proteases (25). For use as a support for immobilization of enzymes, it is very important to effectively control both the textural and surface properties of mesoporous silica. If the molecular size of the enzyme is close to the pore size, it is stated that adsorbate molecules have difficulty in reaching the active regions in the mesoporous channels and diffusion limitations occur. It is noted that this diffusion problem can be solved by using large-pore mesoporous silicas with pore diameters greater than twice the largest enzyme size (12). In the study of Saikia et al. (2019), large pore cubic mesoporous silica SBA-1 MSNs of 500-700 nm functionalized with -COOH were synthesized for papain immobilization. The pore size, specific surface area and pore volume were increased using the pore expanding agent TMB in the reaction mixture. The -COOH functionalized MSNs having a pore size of 5.3 nm exhibited a higher papain adsorption capacity (1138 mg/g) than a pore size of 3.2 nm (995 mg/g). Immobilized papain exhibited higher thermal stability over a wider pH range compared to free papain (12). Kalantari et al. (2017) synthesized octadecylalkyl-modified mesoporous-silica nanoparticles (C18-MSNs) with tunable pore sizes (1.6–13 nm) for lipase immobilization. It has been shown that the pore size slightly larger than the size of the lipase is responsible for the high performance of the immobilized lipase. The optimized C18-MSNs having an average particle size of 60 nm were found to have a high lipase loading capacity of 711 mg / g and a specific activity of 5.23 times higher than that of the free enzyme (26). Kao et al. (2014) tested the activity and stability of lysozyme immobilized in MSNs of various pore sizes by testing secondary and tertiary structures of proteins by methods such as circular dichroism and activity assay. When the pore size was close to the protein size, the activity of lysozyme in immobilizing in the pores of MSNs was found to be higher than pure lysozyme (10).

**Table 1**. Examples of LPMSNs loaded with macromolecular drugs.

| Sample | Size (nm) | Pore Size (nm) | Pore volume ($cm^3/g$) | Specific surface area ($m^2/g$) | Pore expansion agent | Macromolecular drug | Drug loading capacity | Ref. |
|---|---|---|---|---|---|---|---|---|
| LPMSN | 174-207 | 8-10 | 0.6-0.8 | 220-230 | - | Bcl-2 converting peptide | 15%-43% | (6) |
| LPMSN | 230 | 10 | - | 506 | - | Cytochrome-c | 470 μg/mg | (27) |
| LPMSN | 265, 933 | 5.4, 14.5 | 1.82 | 1061 | Mesitylene | Cytochrome-c | 415 mg/g | (28) |
| LPMSN | <150 | 4.6 | 1.14 | 1053 | - | Cytochrome-c | 230 mg/g | (17) |

| | | | | | | | | |
|---|---|---|---|---|---|---|---|---|
| LPMSN | 293 | 16.7 | 1.2 | 315 | - | plasmid-encoding VEGF short hairpin RNA | 26.7 μg/mg | (11) |
| LPMSN | <200 | 13.4, 27.9 | 1.09 | 313 | TMB | Twenty-one-nucleotide (oligo) DNA | 57 μg/mg | (29) |
| LPMSN | 150 | 17.2, 20.5 | 0.46 | 135 | - | pDNA | 9.7 μg/g | (30) |
| XL-MSNs | 180 | 3.6, 30 | 0.7 | 450 | Ethyl acetate | IL-4 | 1030 μg/ mg | (21) |
| Amine-Modified XL-MSNs | 100-200 | 3.2, 25 | 1.05 | 686 | Ethyl acetate | OVA<br>CpG oligonucleotide | ~1000mg/g<br>~80 μg/mg | (22) |
| Large Pore Hollow MSNs | 150-200 | 3.1 | 1.11 | 893.8 | Decane | TRP2<br>HGP100 | 88%<br>20.6% | (31) |
| Amine-Functionalized Hollow Dendritic MSNs | 242 | 20.7 | 2.67 | - | - | IgG,<br>β-galactosidase | 658 μg/ mg<br>391 μg/mg | (19) |
| LPMSN,<br>Hollow Organosilica Nanoparticles | 100<br><br>228-460 | 3-7<br><br>26 | - | 817<br><br>58 | TEB | Pepstatin A | 32%,<br>18% | (20) |
| Mesoporous Organosilica Nanoparticles | 50.75 | 6.2 | 2.19 | 613.9 | - | TAT pDNA | 66.67 μg/mg | (32) |
| Carboxylic Acid Functionalized LPMSNs | 500-700 | 5.3 | 0.88 | 777 | TMB | Papain | 1138 mg/g | (12) |
| PEI-Functionalized Hollow MSNs | 270 | >5.4 | 19.36 | 84.27 | - | GFP-DNA | 37.98 mg/g | (5) |
| Large Pore Magnetic MSNs | 150 | 12 | 1.13 | 411 | Hexane | siRNA targeting polo-like-kinase 1 | 2% | (16) |
| Large Pore Magnetic MSNs | 40-70 | 3.8-6.1 | 0.44-1.54 | 700-1100 | TIPB /Decane | Salmon sperm DNA | 375 mg/g | (23) |
| PEI-Fe-LPMSN | 299 | 4.6, 9.2 | 0.3316 | 217.4 | TMB | Twenty-one-nucleotide (oligo) DNA | 18 μg/mg | (33) |

## 3. Gatekeepers for Controlled Drug Release

Recently, the establishment of stimuli-responsive controlled drug release systems for targeted drug delivery has attracted considerable attention. MSNs are ideal nanocarriers for controlled drug or gene delivery sensitive to stimuli because of their superior properties. A critical step in developing the stimuli-responsive controlled drug release system is to create “gatekeepers” on the surface of MSNs and to block the drug molecules inside the pores with “zero premature release” and trigger the release of drug molecules under specific stimulation (34). These gate-keepers include polymers, cyclodextrin, inorganic nanoparticles and bio-macromolecules developed for efficient capping of the pores (35). The functional design of the pore surface of MSNs with organic or inorganic moieties defined as gatekeepers may regulate the release of guest molecules under the control of external stimuli such as chemicals, temperature, redox reactions and photo-irradiation, or internal stimuli such as pH, redox and enzymes (28).

The gatekeepers are opened only in the presence of specific internal or external stimuli, “zero premature release’’ is achieved before reaching the targeted cancer cells, so that normal cells are not damaged. Various delivery strategies have been reported targeting cancer-specific stimuli, such as low pH, hypoxia, high $H_2O_2$ and glutathione (GSH) levels. In recent years, biomolecule-responsive nanosystems have attracted increasing attention as abundant extracellular enzymes (e.g., phospholipase A, hyaluronidase, lipase, and matrix metalloproteinase) which are highly expressed and active within the tumor microenvironment and could be utilized as drug-delivery stimuli with enhanced selectivity and sensitivity (36).

### 3.1. External Stimuli

#### *3.1.1. Magnetic Field*

The combination of MSNs with magnetic properties has enabled it to be used in areas such as magnetic targeting and magnetic resonance imaging. "Magnetofection" studies are carried out to increase the efficiency of DNA transfection by using magnetic MSNs applied under a magnetic field. Although intensive efforts have been made to develop magnetic LPMSNs for macromolecular drug delivery, there are still some critical limitations to their use. The production of magnetic LPMSNs generally consists of complex multi-stage processes, particle sizes are often too large (> 200 nm) for effective cellular uptake and lead to rapid excretion from the circulation. In addition, low saturation magnetization (<20 emu/g) occurs, often due to the low loading efficiency of the magnetic component. Thus, there is a need for magnetic LPMSNs with small particle size, large open pores, high pore volume, high magnetization density, and controlled release properties for macromolecular drug delivery (16).

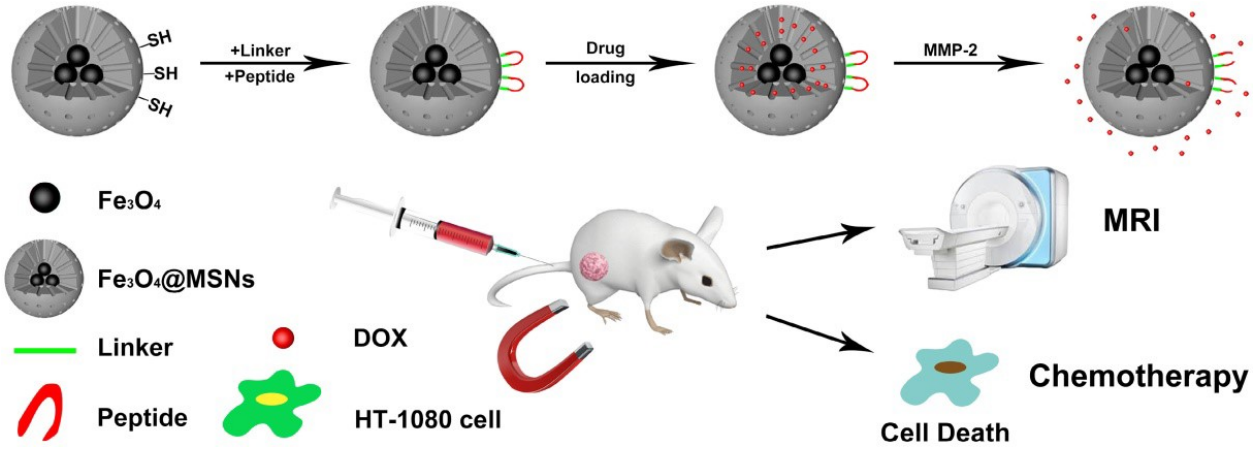


**Figure 3.** Schematic illustration of surface functionalized magnetic MSNs for tumor site specific delivery. Reproduced from Li et.al. (37)

There are many studies showing that magnetic-guided conduction can effectively promote the enrichment of nanocarriers in the tumor site. In a study by Li et al. (2018), mesoporous silica-coated iron oxide-based nanoparticles were synthesized and a peptide sensitive to the MMP-2 enzyme was covalently bound to the surface of nanoparticles to encapsulate doxorubicin in the porous cavities (peptide-$Fe_3O_4$@MSNs/DOX) (Figure 3). Peptide-$Fe_3O_4$@MSNs/DOX were cultured with NIH/3T3 and HT1080 cells to test the specificity of normal cells and cancer cells. The cell viability after 24 hours was found still approximately 80% in NIH/3T3 cells, while it was about 50% in HT-1080 cells. In tumor bearing mice, uptake of peptide-$Fe_3O_4$@MSNs/DOX into tumor cells by passive targeting was found to be much lower than that treated with magnet. The *in vivo* peptide-$Fe_3O_4$@MSNs/DOX and magnet-treated group was found to have the smallest tumor size, indicating successful suppression of tumor growth. This phenomenon has demonstrated that magnetic-guided conduction can effectively promote the enrichment of nanocarriers in the tumor site (37). Portilho et al. (2018) developed an intelligent delivery system, based on trastuzumab-loaded radiolabeled magnetic core MSNs for *in vivo* breast cancer imaging and treatment. The results showed that nanoparticles were 58.9 nm in size with a specific surface area of 872 $m^2$/g, pore volume of 0.85 $cm^3$/g and a pore diameter of 3.15 nm. Entrapment efficiency of transtuzumab into the magnetic core MSNs was found as 97.5%. Biodistribution studies showed systemic uptake of 7.5% and intralesional tumor uptake of 97.37%, whereas less than 3% were absorbed by healthy tissues. During a 6-hour post-injection period, a tumor-limited barrier was not crossed, which supported its use as intralesional nanodrug (38).

Magnetic MSNs have been used for gene delivery to cancer cells. Xiong et.al. (2016) developed a large pore magnetic core–shell silica nanoparticle for small interfering RNA (siRNA) delivery. These nanoparticles were produced by coating super-paramagnetic magnetite nanocrystal clusters with radial large-pore mesoporous silica. To prepare large mesopores, hexane (an organic additive) was used as a pore expander. The amine functionalized nanoparticles were found to have small particle sizes around 150 nm, large radial mesopores of 12 nm and magnetization of 25 emu/g. Thus, these nanoparticles were found to have both siRNA loading capacity of 2% and strong magnetic response under an external magnetic field. The tannic acid coating also increased the dispersion stability of the siRNA-loaded carrier and provided a pH sensitive release. Using tannic acid coated magnetic silica nanoparticles as the carrier, functional siRNA was successfully delivered to the cytoplasm of human osteosarcoma cancer cells and the delivery was

significantly increased with the help of an external magnetic field (16). In another study, Hartono et.al. (2014) reported the synthesis of LPMSNs loaded with iron oxide and covalently modified by polyethyleneimine (PEI) as a carrier for gene delivery. The functionalized LPMSNs were found to have a particle size of 300 nm and a large cavity size of 9.2 nm with an entrance size of 4.6 nm. The amount of oligo-DNA adsorbed by functionalized LPMSNs was obtained as 18 μg/mg. Cellular uptake studies showed a 12% intensity increase under magnetic therapy when compared to the group without application of a magnetic field. The functionalized LPMSNs delivered siRNA–PLK1 effectively into osteosarcoma cancer cells resulting in a higher cell viability inhibition of 80%, compared to the 50% reduction when the same siRNA dose was administered by a commercial product, oligofectamine (33).

The surface of magnetic MSNs can be functionalized with aptamers and targeted to cancer cells. Siminzar et.al. (2019) designed mucin-1 (MUC-1) conjugated mesoporous silica magnetic nanoparticles for the targeted delivery of doxorubicin to breast cancer cells. Superparamagnetic iron oxide nanoparticles (SPIONs) were synthesized using thermal decomposition technique and then coated with mesoporous silica to modify their biocompatibility and reduce undesired cytotoxic effects. Doxorubicin was then loaded into the silica porous structures, which was then grafted with 5'-amine-modified MUC-1 aptamers. Transmission electron microscopy and particle size analysis showed spherical and monodisperse nanoparticles with a size range of 5–27 nm. MUC-1 grafted SPIONs coated with mesoporous silica were applied to MUC-1-positive MCF-7 cells, resulting in higher cytotoxicity and higher uptake (39). In another study, Sakhtianchi et.al. (2019) synthesized an aptamer-functionalized PEG-coated SPION/mesoporous silica core-shell nanoparticle for simultaneous cancer targeted therapy and magnetic resonance imaging. Doxorubicin was loaded into the MSNs, which were then coated with di-carboxylic acid functionalized polyethylene glycol and AS1411 aptamers were covalently attached to MSNs. The synthesized nanoparticles were found to be 89 nm in size and the doxorubicin loading degree was 13.17%. The cytotoxicity assay demonstrated a significantly higher toxicity of decorated MSNs to MCF7 cells. Aptamer decorated MSNs induced highest signal intensity reduction in T2-weighted images during *in vitro* MRI assay (40).

### *3.1.2 Photodynamic therapy*

Photodynamic therapy (PDT) is a non-invasive and innovative cancer therapy based on the photodynamic effect. In combination with light and molecular oxygen, photosensitizers, which are applied during PDT, produce reactive oxygen species (ROS) to destroy tumor tissues and cells. PDT exhibits spatiotemporal selectivity because ROS production occurs in the light-exposed region, and the resulting chemical processes take place within about 50 nm of this location. In addition to this inherent selectivity, PDT has demonstrated the advantages of non-invasivity, having a relatively broad-spectrum anticancer effect, allowing repeated treatments without initiating resistance, and providing an immune response. Besides its advantages, the typical PDT approach suffers the drawback that patients must stay in the dark for a long time (usually 4−6 weeks) after treatment, so that the photosensitizers can be removed from the body. Otherwise, photosensitivity of the skin and damage to other tissues may occur (41).

Er et.al. (2018) synthesized MSNs targeted with cetixumab, a monoclonal antibody that targets the Epidermal Growth Factor Receptor (EGFR) and loaded with zinc(II) 2,3,9,10,16,17,23,24-octa(tert-butylphenoxy))phthalocyaninato(2-)-N29,N30,N31,N32 (ZnPcOBP) against pancreatic cancer cells to determine the singlet oxygen production, intracellular uptake, and PDT potential *in vitro*. Upon irradiation, concentration and light fluence-dependent decrease in cell viability was observed in pancreatic cell lines. The results in this study demonstrated that nanoparticles coated with PEG and cetuximab could be an efficient vehicle for delivery of the photosensitizer ZnPcOBP to tumoral pancreatic cells with targeted high

EGFR expression (42). Li et.al. (2019) developed a sequential protein-responsive activatable photosensitizer ($PcC_4$-MSN-$O_1$) based on zinc(II) phthalocyanine derivative ($PcC_4$)-entrapped MSNs and a wrapping DNA ($O_1$) as a biogate. First, MSNs with particle sizes of about 50 nm were synthesized because this size range is claimed to be preferred for tumor passive deposition through the EPR effect. Second, the MSNs were modified with APTES, resulting in positively charged surfaces. Finally, MSN-$NH_2$ were loaded with $PcC_4$ and then sealed with the negatively charged $O_1$ to form a $PcC_4$-MSN-$O_1$ nanosystem. In this nanosystem, the loading of $PcC_4$ was calculated as 77.6 nmol/mg MSN-$NH_2$, and the adsorption amount of $O_1$ was calculated as 0.3 µmol/g $PcC_4$-MSN. The cytotoxicity of PcC4-MSN-$O_1$ upon illumination with white light was tested. $PcC_4$-MSN-$O_1$ exhibited concentration-dependent phototoxicity against HeLa cells (telomerase overexpressed) but not show significant phototoxicity against normal cells (HEK-293) under the same conditions indicated its selective effect on cancer cells. They also investigated the *in vivo* PDT efficacy of $PcC_4$-MSN-$O_1$ on tumor-bearing mice and compared with the control group (laser irradiation only), the group treated with $PcC_4$-MSN-$O_1$ exhibited significant deposition of formulation in HeLa tumors and a significant inhibition in tumor growth in the presence laser irradiation (41).

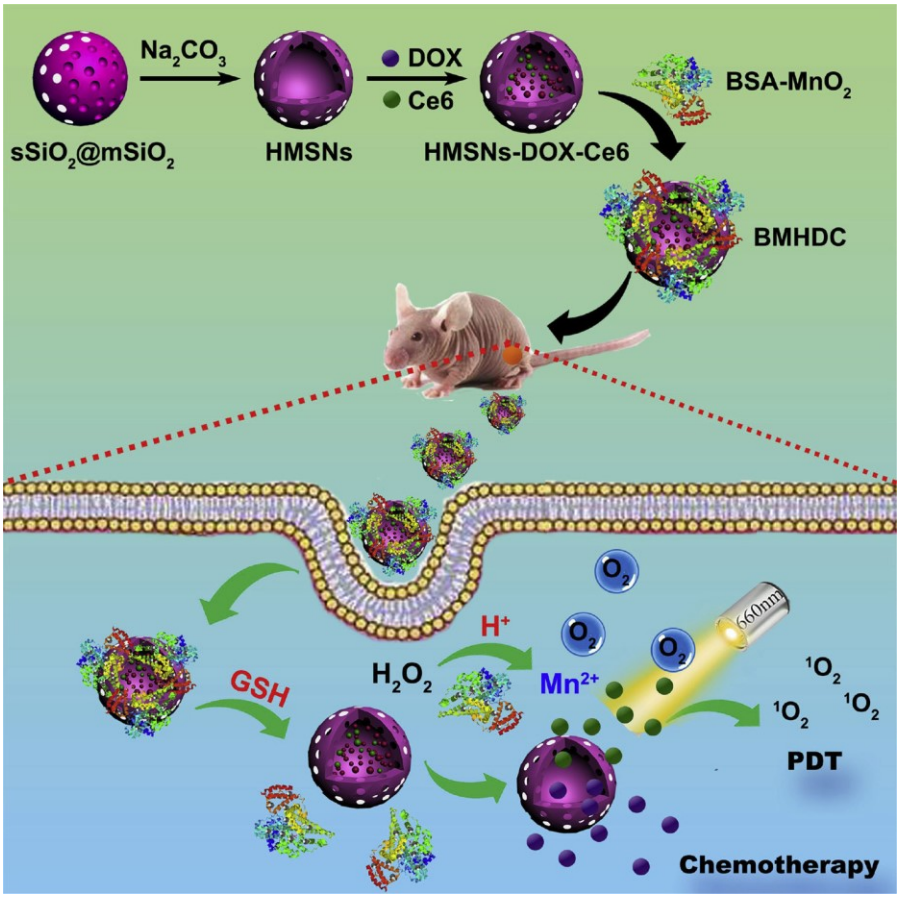


**Figure 4**. Schematic representation of drug release from MSNs based on the photodynamic effect. Reproduced from Fang et.al. (43)

In another study, Fang et al. (2019) designed a hollow MSN gated with BSA integrated manganese dioxide nanoparticles (BSA-$Mn0_2$) for both chemotherapy and $O_2$-induced photodynamic therapy. The BSA-$MnO_2$ nanoparticles were then attached to the surface of hollow mesoporous silica nanospheres (BMHDC) co-loaded with chemotherapeutic drug doxorubicin and photosensitizer chloride e6 (Ce6) by formation of disulfide bonds. BSA-$MnO_2$ was used not only as a gatekeeper to prevent early release of drugs from

hollow MSNs, but also as an oxygen generator to eliminate tumor hypoxia. Furthermore, the BSA component has also been noted to increase the stealthiness of nanoparticles during blood circulation. Under acidic pH and GSH, decomposition of $MnO_2$ caused the gatekeeper to open and simultaneously release doxorubicin and Ce6 (Figure 4). In addition, $O_2$ generation supported the kinetics of $O_2$ production to improve PDT outcomes. The produced BMHDC nanoplatform was able to effectively limit human cervical carcinoma through synergistic PDT and chemotherapy demonstrated in both *in vitro* and *in vivo* experiments (43).

### *3.1.3. Ultrasound*

The surface of the MSNs can be functionalized to control cargo release by ultrasound effect. Paris et.al. (2019) demonstrated the possibility of inducing gene transfection using ultrasound-responsive MSNs, without generating significant toxicity to the Decidua derived Mesenchymal Stem Cells (DMSCs), by using a PEI coating. Ultrasound-responsive MSNs were obtained by grafting the polymeric gate poly-(2-(2-methoxyethoxy) ethylmethacrylate-co-2-tetrahydropyranyl methacrylate) to MSNs. When exposed to ultrasound, the monomer tetrahydropyranyl methacrylate in the polymeric coating is converted into a much more hydrophilic monomer (methacrylic acid). This change modifies the overall hydrophilicity of the system and induces a conformational change of the polymeric gate by exposing the nanoparticle pores to the environment and enabling cargo release (Figure 5). This developed nonviral transfection agent was used to transfect DMSCs with an expression plasmid comprising two suicide genes consisting of the sequences for cytosine deaminase and uracil phosphoribosyl transferase, which provided them the capability of converting non-toxic 5-Fluorocytosine into toxic 5-Fluorouridine monophosphate. It has been found that DMSCs transfected with suicide genes can induce cell death in co-cultured NMU cancer cells when exposed to non-toxic prodrug 5-Fluorocytosine (44).

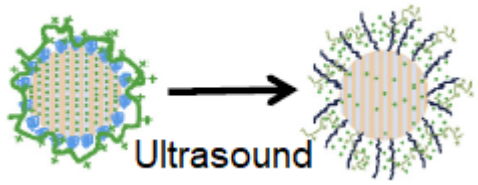


**Figure 5.** Schematic representation of MSN before and after ultrasound treatment. Reproduced from Paris et.al. (44)

## 3.2. Internal Stimuli

### *3.2.1. Release based on pH*

One of the most commonly used stimulants in triggered drug release is pH. In cancer drug delivery, drug carriers coated with gatekeepers can prevent drug release in the bloodstream, but when the nanoparticle reaches the tumor microenvironment by EPR and/or enters the target cell via endocytosis, drug release from the nanocarriers is triggered either around the tumor where pH is lower than in healthy tissue or intracellularly. Because of the abundance of $H^+$ in the endosomes, the pH in this cellular organ where nanoparticles reside after endocytosis is estimated to be pH 5.0 and is lower than the cytosolic medium of the cell (45).

Many substances and polymers with different chemical structures have been utilized for pH-sensitive functionalization of MSNs. In the study of Shen et.al (2019) benzimidazole-functionalized MSN was prepared to provide pH-triggered release of doxorubicin. β-cyclodextrin (β-CD) was used as a gatekeeper for encapsulated doxorubicin. Release of doxorubicin sensitive to pH was confirmed by *in vitro* release experiments (46). Xiong et al. (2016) developed a large pore magnetic core-shell silica nanoparticle for siRNA delivery. The acid-liable surface coating of tannic acid was reported to act simultaneously as a pore capping agent for effective protection of siRNA and as a pH-sensitive switch for intracellular release of siRNA (16). Zahiri et.al. (2019) developed a new pH responsive formulation in which polycarboxylic acid dextran was electrostatically adsorbed to the amine groups on the surface of doxorubicin loaded dendritic MSNs. They claimed that under physiological condition (pH 7.4), the silica channels were coated and sealed by dextran polysaccharides but positively charged hydrogen ions in the citrate buffer (pH 5.4) interacted with carboxylate group of dextran and became protonated. Therefore, it has been noted that electrostatic interaction between surface amine groups and dextran carboxylate groups could be compromised by a competitive binding with $H^+$, resulting in the release of doxorubicin (45). Liu et al. (2019) introduced a biocompatible, simply structured and tumor-acidic environmentally sensitive drug delivery system by using $CaCO_3$ as a gatekeeper and cloaking cancer cell membrane on MSNs. It has been reported that the synthesized MSNs are monodisperse nanoparticles having a size of about 100 nm and that the modification of the surface does not affect the morphology of the nanoparticles. Negligible early release at pH 7.4 and rapid release under tumor acidic medium was confirmed. Furthermore, doxorubicin loaded $CaCO_3$ capped MSNs showed a positive anti-tumor effect in the LNCaP-AI tumor model, evidenced by significant tumor growth delay, destruction of tumor cells and reduced tumor cell proliferation (47). Kuang et.al. (2019) prepared doxorubicin hydrochloride loaded MSNs and coated by ZnO and subsequently poly-L-lysine (PLL) and 2,3-dimethylmaleic anhydride functionalized PLL (PLL(DMA)) was adsorbed on the surface. The outer part of the carriers was negative charged PLL(DMA) and due to the charge-reversal property, the carriers were found to be difficult to uptake cellularly at pH 7.4, but were able to enter the HeLa cells more easily after accumulation in weakly acidic tumor tissues (pH 6.5), as the hydrolysis of β-carboxylic amide revealed the positive charged PLL. The lower pH in the cancer cell (4.5–6.5) has caused the dissolution of the "cap" ZnO to release doxorubicin for cellular apoptosis (48).

### *3.2.2. Release based on Glutathione*

Recently, glutathione (GSH) has been widely exploited to develop a stimulus-sensitive system by breaking down the disulfide bond in the structures using the large difference of its concentration between extracellular (2−10 μM) and intracellular (2−10 mM) conditions. Importantly, the GSH concentration in cancer cells was found to be several times higher than normal cells, and this could be utilized by different drug delivery systems for selective cancer treatment (49). Yang et al. (2016) designed disulfide bond bridged and large-pore MSNs for intracellular RNase A delivery. These disulfide bond bridged MSNs exhibited a GSH-sensitive degradation behavior that exhibited a higher rate of degradation in cancer cells but a lower rate in normal cells (49). Wu et al. (2016) formulated a redox-sensitive gene release by decorating poly (β-amino esters) via a disulfide binder based on the large pore size of HMONs (hollow mesoporous organosilica nanoparticles). These redox-sensitive intelligent nanocarriers were used to co-deliver P-glycoproteins (P-gp) modulator siRNA and anticancer drug doxorubicin to reverse the multidrug resistance of breast cancer cells both *in vitro* and *in vivo* (18).

Many studies have shown that GSH-sensitive release is combined with other stimulants to give MSN dual-sensitive properties. Shao et al. (2018) developed oxidative / redox dual-responsive large-pore organosilica nanoparticles to deliver RNase A for cancer treatment. These diselenide-bridged MSNs were able to load cytotoxic RNase A into the internal pores of 8 to 10 nm by electrostatic interaction. RNase A-loaded MSNs

exhibited oxidative / redox dual-responsive protein release behavior and improved *in vitro* and *in vivo* anti-cancer activity with low systemic toxicity (50). In the study of Zhang et.al. (2019), a functionalized dual-sensitive MSN formulation was prepared for both redox-responsive drug release and enzyme-responsive drug release (Figure 6). Apoptotic peptide $(KLAKLAK)_2$ was attached to the MSN surface by disulfide bonds and was expected to release by responding to GSH in tumor cells. Then they chose reductive agent dithiothreitol (DTT) as an alternative to GSH, to mimic reductive environment inside cells. The release rate of apoptotic peptide from the MSN-SS-KLA with DTT was found to be significantly faster than that without DTT, and the drug release rate increased as DTT concentration increased. This is due to the cleavage of the disulfide bonds between KLA and MSN under reductive conditions. To investigate the effect of enzyme on drug release, BSA was used as the outer layer of the MSN-based drug carrier. Since trypsin is capable of degrading BSA, *in vitro* release experiments containing trypsin at different concentrations were performed. Drug release rate from the doxorubicin loaded MSN-SS-KLA/BSA was found to be significantly faster with trypsin than that without trypsin. Therefore, they concluded that a dual-sensitive drug delivery system (doxorubicin@MSN-SS-KLA/BSA) capable of achieving the expected off-on release behavior has great potential for antitumor application as smart carriers (51).

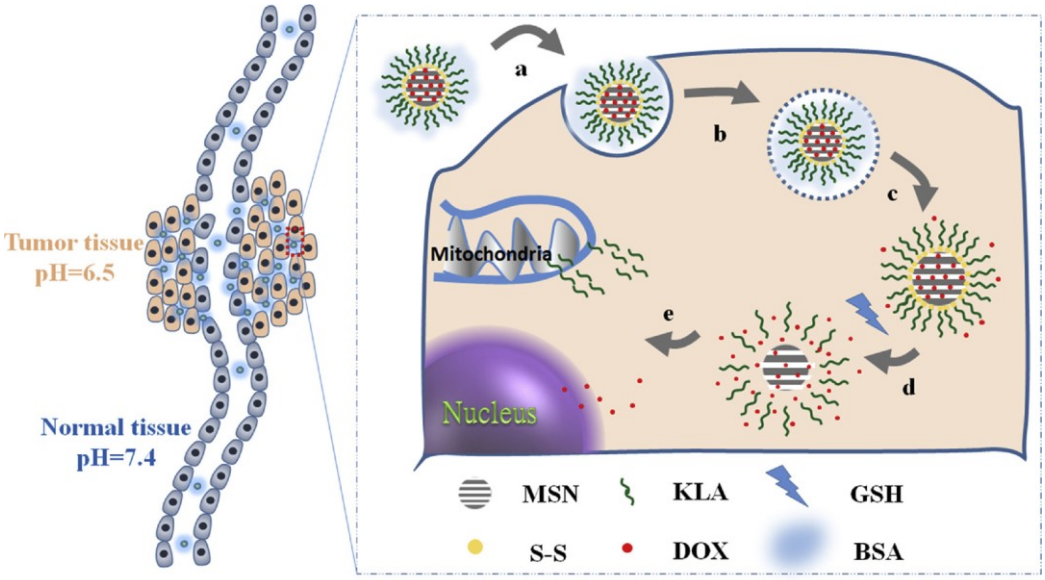


**Figure 6.** The cleavage of disulfide bonds by the highly concentrated GSH in the cytoplasm of tumor tissue leading to the release of chemotherapeutics. Reproduced from Zhang et.al. (51)

### *3.2.3 Release based on biomolecular recognition*

Recently, biomolecules such as antigen-antibody interaction, hybridization of single-stranded DNA, and enzymes have been used as gatekeepers to control drug release. The development of enzyme-gated MSN makes it possible to prepare specific sequences that can provide fine selectivity in the design of advanced gatekeepers. The enzymes may act as a primary sensor to detect the presence of target compounds to be recognized as the INPUT signal and may further catalyze their conversion into a specific stimulus capable of "opening" the gates. These enzymes can be used as binary systems as control elements and gate molecules or can be immobilized as a control unit (52).

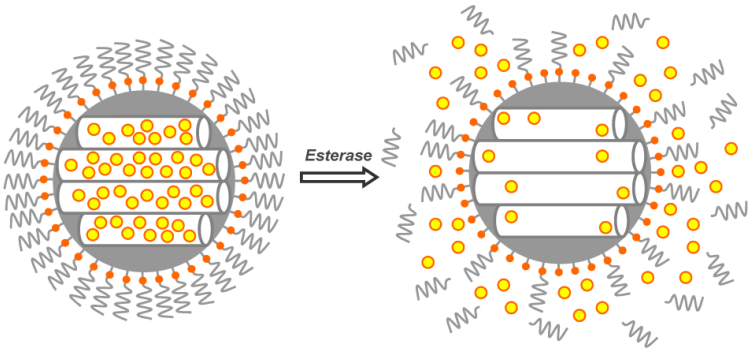


**Figure 7.** Hydrolysis of the ester bond in the presence of a specific enzyme (esterase) and the release of the entrapped cargo. Reproduced from Agostini et.al. (53)

Agostini et.al. (2012) prepared an ethylene glycol-capped hybrid material for the controlled release of molecules in the presence of esterase enzyme. The resulting organic–inorganic hybrid solid S1 was synthesized by a two-step procedure. In the first step, the pores of an inorganic MCM-41 support (in the form of nanoparticles) were loaded with the ruthenium complex, and then, in the second step, the pore outlets were functionalized with ester glycol moieties that acted as molecular caps. In the absence of an enzyme, release of the complex from aqueous S1 suspensions at pH 8.0 was inhibited due to the steric barrier imposed by the bulky ester glycol moieties. Upon addition of esterase enzyme, delivery of the ruthenium complex was observed due to enzymatic hydrolysis of the ester bond in the bounded ester glycol derivative which induced the release of oligo (ethylene glycol) fragments. Hydrolysis of the ester bond allowed the release of the entrapped cargo (Figure 7). The S1 nanoparticles were not toxic for cells, as demonstrated by cell viability assays with HeLa and MCF-7 cell lines and were found to be associated with lysosomes as demonstrated by confocal microscopy. However, cells treated with the cytotoxic drug camptothecin loaded S1 nanoparticles, underwent cell death as a result of cellular internalization and subsequent cellular enzyme-mediated hydrolysis followed by opening of the molecular gate that induces the release of camptothecin (53).

Nanosystems responsive to tumor-specific enzymes are considered as a highly attractive approach for intracellular drug release in targeted cancer therapy. The most important point for successful chemo-responsive release is to select the appropriate combination of enzyme media and capping agent to trigger the drug release. In this context, Qiao et.al. (2019) developed an enzyme-sensitive drug delivery system that targets the specific intracellular microenvironment in tumor tissues and releases loaded therapeutic agents only in the presence of indoleamine 2,3-dioxygenase 1 (IDO1) enzyme. MSNs were capped with tryptophan mediated cucurbit[8]uril complex together with $Fe_3O_4$ to minimize the premature drug leakage to deliver the payload on demand in target tissue. The supramolecular interaction between tryptophan and cucurbit[8]uril is impaired in the presence of IDO1 enzymes which are overexpressed in various cancer cells and intracellular release of therapeutics exclusively in tumor cell. The MTT and FACS results confirmed that drug release is triggered only in the presence of the highly selective IDO1 enzyme and induces significant cytotoxicity against HepG2 cells as well as the superior antitumor effects *in vivo* (36). In another study, Yu et.al. (2018) constructed a $Mg^{2+}$-dependent DNAzyme functionalized hollow MSNs loading with anticancer drug doxorubicin. $Mg^{2+}$-dependent DNAzyme on the surface of HMSNs nanopores acted as a gatekeeper locking the doxorubicin in the nanostructure of HMSNs and unlocking the nanopores of hollow MSNs to release doxorubicin when triggered by $Mg^{2+}$ ions. These $Mg^{2+}$ ions originated from the biodegradation of hollow MSNs that release $Mg^{2+}$ ions in slightly acidic microenvironment of tumor tissues. In addition, the anticancer activity of chemotherapeutic drugs assisted by these biodegradable smart nano-carriers has been increased. Tumor growth of $Mg^{2+}$ dependent DNAzyme functionalized hollow

MSNs-treated mice compared to control and free doxorubicin groups showed enhanced tumor growth inhibition efficiency and tumor-suppressing effect of functional hollow MSNs loaded with anticancer drug doxorubicin could reach up to 68.75 % (9). Although different strategies have been developed to achieve chemo-responsive release, particularly in the tumor region, further studies are needed to understand biodistribution and bioaccumulation of these systems and reduce immunogenic responses.

## 4. Macromolecular Drug Delivery by MSNs for Cancer Diagnosis and Therapy

Cancer has been one of the leading causes of death worldwide for decades. Traditional cancer chemotherapy is still a common treatment, but toxicity problems are inevitable due to the similarity between healthy human and cancerous cells. Cancer is generally believed to be a special site with unique microenvironment with a low pH, high GSH concentration, hypoxia and tumor-specific enzymes. Therefore, the design of therapeutic nanoplatforms with novel properties that can respond to specific characteristics of the tumor microenvironment has been considered a promising strategy to achieve the desired therapeutic efficacy. In addition, nanoplatforms with flexible properties that can increase blood circulation time and their accumulation in tumors are highly desirable, especially for cancer nanoproducts (43).

### 4.1. Peptide/Protein Delivery

Intracellular protein delivery allows biomedical applications such as cancer therapy, vaccination and administration of enzyme-based therapeutics. However, therapeutic proteins are susceptible to high and low pH environments or proteolysis and denaturation, limiting their activity in the body (27, 54). Therefore, there is a need for novel delivery systems capable of delivering therapeutic proteins to the site of action while maintaining their stability. In this context, the use of MSNs for intracellular protein delivery has many advantages. The large pore volumes of MSNs (>1 $cm^3/g$) allow for loading a measurable amount of protein into the particles. The chemically and mechanically stable inorganic oxide framework of MSNs protects protein molecules from exposure to proteases and denaturation chemicals. In many applications, such as cancer therapy and immunotherapy, protein therapeutics need to function within cells, however bare protein cannot automatically cross cell membranes (55). MSNs have been found to be advantageous not only for the entry of proteins into cells, but also for their release into the cytoplasm (28).

There are many studies investigating the use of therapeutic proteins in cancer imaging and therapy through MSNs. Xu et.al. (2019) prepared arginine-glycine-aspartic acid-N-ε-acryllysine (RGD-Acrk) conjugated MSNs as potential fluorescence imaging nanoprobes of breast cancer tissues *in vivo*. RGD peptides are known to selectively bind to αVβ3/αVβ5 integrin proteins overexpressed on the surface of breast cancer cells. *In vitro* confocal and fluorescent imaging showed that these nanoprobes have good binding affinity for the surfaces of breast cancer cells (4T1), resulted in the internalization and accumulation in the cytoplasm of 4T1 cells. RGD-Acrk conjugated MSN nanoprobe was applied *in vivo* to detect tumors of breast cancer mice. It has been noted that these nanoprobes are non-toxic, targeted fluorescent probes that selectively accumulate in cancer cells and tissues for early detection and monitoring of tumor growth *in vivo* (55). MSNs with large pores and different geometries have been tested for higher loading of peptides/proteins and increased uptake and cytotoxicity of cancer cells. Rahmani et al. (2019) synthesized LPMSNs and hollow MSNs and loaded pepstatin A into both formulations, with a loading efficiency of 32% and 18%, respectively. TEB was used as pore expanding agent in these formulations. Although LPMSNs have higher loading capacity, pepstatin A-loaded LPMSNs lead to 20% cell death in MCF-7 breast cancer cells, while approximately 60% cell death is observed in hollow MSNs. It has been suggested that this may be due to the release of pepstatin A in cancer cells prior to endocytosis and

the binding of pepstatin A to HOSNP with a stronger interaction (20). In another study, a new type of MSNs featuring a cuboidal-like geometry and large pores (10 ± 1 nm) was synthesized by Yang et.al. (2017). The maximum Cytochrome-c loading capacity of these cuboidal MSNs was determined to be 470 µg/mg MSNs. To increase the colloidal stability, MSNs/cytC were decorated with a fusogenic lipid bilayer and the hydrodynamic diameter observed by dynamic light scattering of the nanoparticles was found to be 230 nm. The lipid bilayer acted as a physical barrier and reduced the early release of cytC, thereby retained the protein better in MSNs. The delivery and bioactivity of cytC using lipid bilayer-coated MSNs resulted in 55% of apoptosis after 48 hours, due to increased uptake and release of cytC into the cytosol of the HeLa cells (27). Gu et.al. (2013) synthesized monodispersed MSNs using cationic surfactants as templating agents, neutral amine of N, N-dimethylhexadecylamine as a pore size mediator and tri-block copolymer of F127 as a particle growth inhibitor/dispersant. The obtained MSNs exhibited a highly ordered mesostructure and tunable pore diameter up to 4.6 nm and monodispersed particle sizes less than 150 nm. A model protein, cytC was loaded (230 mg/g) in the resultant MSNs. To demonstrate their potential as a protein delivery vehicle, the uptake of the cytC-MSNs by HeLa cancer cells was investigated and it was determined that MSNs were efficiently internalized into cancer cells and could escape from endosomes (17).

It is important to evaluate the pore width and particle size together for the efficient uptake of macromolecules by the cells. Slowing et.al. (2007), synthesized a MCM-41-type MSN with a large pore diameter by adding a pore-expander TMB to a CTAB-templated synthesis. The BJH method yielded two pore size distributions centered on 5.4 nm (major peak) and 14.5 nm (minor). Two different particle size distributions (265 and 933 nm) were measured by dynamic light scattering. The cytochrome c-encapsulated MSNs were internalized by living human cervical cancer cells (HeLa) and the protein could be released into the cytoplasm. The uptake of MSNs observed in this study was found lower than previously observed for MSNs with the smaller pore size. This difference in uptake efficiency was mainly attributed to the difference in particle size, since the smaller pore MSNs has an average size around 150 nm, whereas the pore-enlarged MSNs are larger than that (28). This is the first known example of intracellular protein delivery by MSNs.

A unique advantage of MSNs is the nanoparticle morphology with two independent surfaces (Fig. 1). MSNs have an inner pore surface and an outer surface that can not only serve for different critical functions in the biomacromolecular delivery process (see Figure 8) but can also be selectively and independently functionalized. Thus, chemical and biological material can be applied together using these surfaces of MSN. For example, Zhang et.al. (2019) designed a multifunctional MSNs for sub-cellular co-delivery of drug and therapeutic peptide to tumor cells. Firstly, a kind of cell apoptosis peptide $(KLAKLAK)_2$ (KLA) was anchored on the MSN surface to help the MSN drug carrier escape from endosome after being internalized by tumor cells and release the loaded drug in the cytoplasm. The anticancer drug doxorubicin hydrochloride was then loaded into the pores of MSNs. Then, the drug loaded MSNs were coated with BSA to achieve a biologically stable MSN based drug delivery system for cancer synergetic therapy and were able to keep well dispersed in serum for more than 24 hours. After accumulating by EPR effect in the tumor site, the KLA-peptide anchored doxorubicin-loaded BSA coated MSNs were able to be effectively phagocytosed by HeLa cells and release apoptotic peptide KLA with doxorubicin, which simultaneously respond to reductive stimulus inside the cells. *In vitro* results showed that the resulting MSN formulation exhibited better inhibition on HeLa cells compared to pure doxorubicin; this demonstrated the success of co-delivery of KLA and doxorubicin to achieve synergetic cancer therapy (51). In the study of Xu et al. (2018), hydroxyl, amine, thiol and carboxyl-functionalized MSNs loaded with Bcl-2-converting peptide were synthesized by different surface functionality to treat multidrug-resistant cancer cells. The resulting large pore (8-10 nm) MSNs having a small particle size of 174-207 nm exhibited a high Bcl-2-converting peptide loading

efficiency of over 40%, especially in those modified with the thiol group. In addition, the amine-modified surface of MSNs has been shown to have a greater effect on the cell apoptosis inducing effects of peptide compared to others (6). Tambe et.al. (2018) synthesized PEG and triptorelin ligand-conjugated MSNs and characterized them for targeted drug delivery to GnRH-overexpressing cancer cells. Internalization studies showed higher uptake and significant cytotoxicity of doxorubicin-loaded targeted MSNs as compared to doxorubicin-loaded bare MSNs in breast (MCF-7) and prostate (LNCaP) cancer cell lines (56). Bhattacharyya et.al. (2012) synthesized poly (ethylene glycol) (PEG)-coated MSNs with an average particle size of 120 nm containing trypsin inhibitor (TI), a model protein molecule for growth factors. The pore size of the MSNs was expanded by a hydrothermal treatment prior to TI incorporation. 16 % loading of TI was achieved for pore-expanded MSNs. In the PEG-coated MSNs, zero order release was achieved for 4 weeks (57).

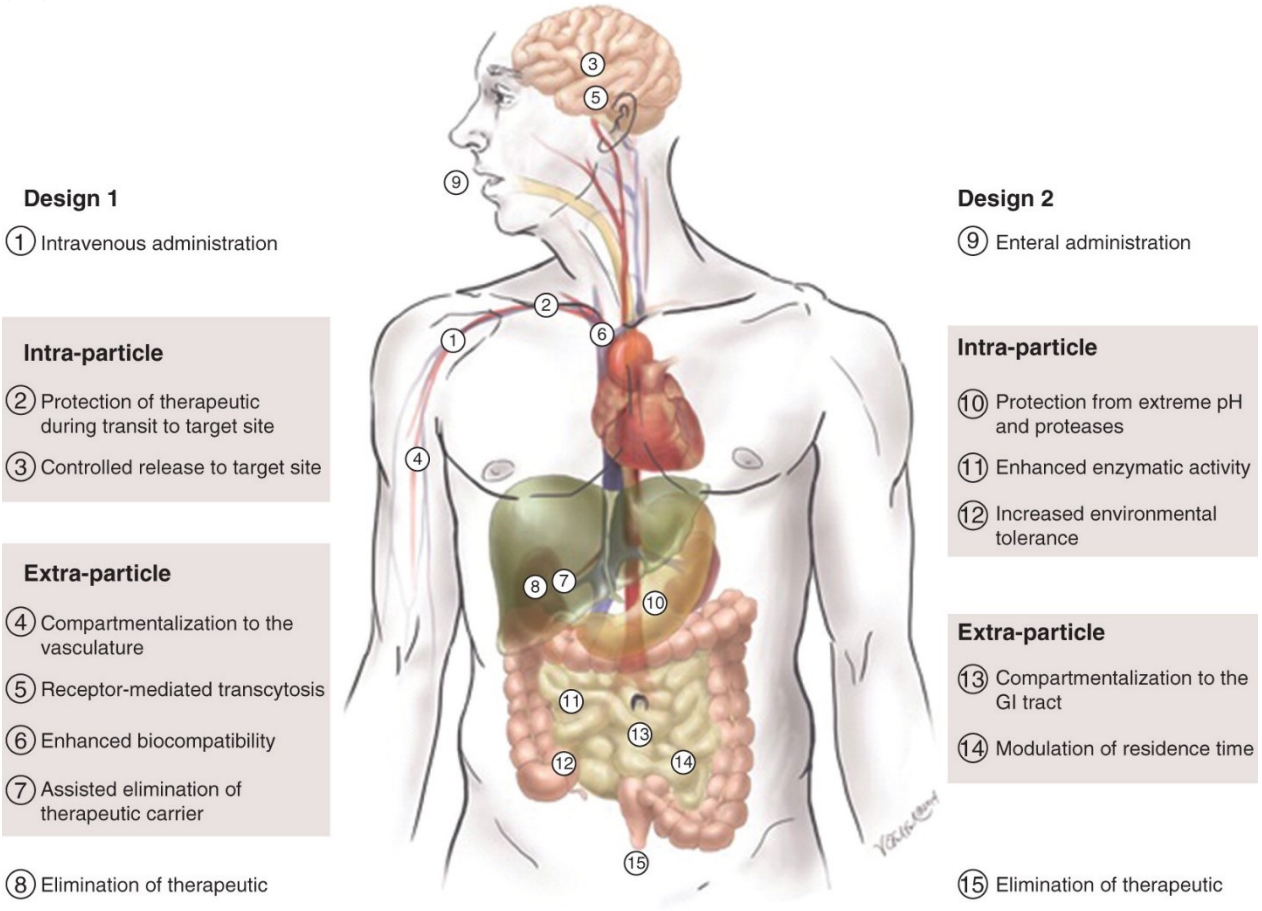


**Figure 8.** Illustration of how the inner and outer MSN surfaces can be of benefit during the delivery process considering two different routes of administration (IV/parenteral and oral/enteral). Reproduced with permission © 2019 Virginia E. Fulford.

As mentioned in the studies above, MSNs allow various modifications to suitably protect the protein structure against physiological conditions. However, although MSN pores are enlarged so that proteins can be loaded, for larger proteins, there is still a size limit. Only small proteins can be loaded successfully because larger ones will not fit in the pores. In this respect, the development of MSN's properties for protein delivery is an area that needs to be improved.

### 4.2. Gene Delivery

Gene therapy is a promising strategy to treat cancer and other diseases. However, the transfer of a desired gene into host cell nucleus to treat genetic disorders is a complex process with various limitations. Successful gene delivery requires an efficient system to deliver genes to specific cells because naked nucleic acids alone can be rapidly degraded by endogenous nucleases and can be difficult to penetrate through cell membranes. Therefore, an effective gene delivery vector should be able to load a sufficient number of genes, provide a protective environment, and effectively penetrate into cells. In addition, the preparation for an ideal gene carrier should be easy and the carrier system should not be toxic (5).

#### 4.2.1. *p*DNA Delivery

MSNs usually have a relatively small 2-3 nm pore size that is not applicable for gene loading and delivery. However, it has been reported that MSNs with pores larger than 5.4 nm are favorable for the absorption of DNA (2000 bp) into the internal pores (58). The benefit of using LPMSNs as a DNA carrier is to achieve high DNA loading and to provide enhanced protection of DNA against DNase degradation. However, the successful application of LPMSNs for delivery of nucleic acid-based drugs requires surface modification of the silica to produce enough binding affinity for the negatively charged nucleic acids. A variety of techniques have been applied to introduce positively charged functional groups in silica materials, either through noncovalent interactions or by covalent bonding. Amino-silanes and polycation polymers have been widely used as chemical agents for modifying silica surfaces (29). However, there is still a need to develop a simple synthetic methodology for producing MSNs with large pore sizes and ultra-small particle sizes for intranuclear gene delivery as well as high biocompatibility and transfection efficiency (32).

Numerous studies have been conducted for cancer therapy by introducing genes through MSNs. Niu et.al. (2014) developed monodispersed LPMSNs with ordered, accessible and interconnected pore channels, and smaller particle dimensions by employing common polystyrene- b -poly (acrylic acid) as pore template and CTAB as structure-stabilizing agent. By controlling the amount of CTAB added, LPMSNs with different mesostructures (hexagonal, cubic and lamellar) were synthesized. In addition, the morphology of the MSNs varied from large-pore MSNs to hollow MSNs using block copolymers having shorter or longer PAA lengths as pore templates. The well-defined and monodisperse nanospheres with a hydrodynamic diameter of 293 nm and mesopore diameter of ∼16.7 nm were produced. Finally, to assess the loading capacity of amino-functionalized LPMSNs, the plasmid encoding VEGF short hairpin RNA (pDNA) was selected as model gene. The loading amount of the pDNA was found to be 26.7 μg/mg. The transfection efficiency of pDNA loaded LPMSNs into human hepatocarcinoma cell line (SMMC-7721 cells), and *in vivo* tumor gene therapy in SMMC-7721 tumor-bearing mice was also investigated. Compared to the control group, the VEGF mRNA level was down-regulated in cells treated with pDNA loaded amine-modified LPMSNs, which showed remarkable down-regulation ability in targeting the VEGF gene. The pDNA loaded amine-modified LPMSN treated mice significantly reduced tumor volumes by 47% in 21 days, as compared to the control group. It has been concluded that amine-modified LPMSNs could act as effective plasmid carriers to knockdown VEGF both *in vitro* and *in vivo*, and demonstrate their potential for application in future cancer treatment (11). In another study, Chang et.al. (2019) developed MSNs that can deliver a sleeping beauty system to permanently integrate the asparaginase gene into the genome of human lung adenocarcinoma cells. The Sleeping Beauty (SB) transposon system is a non-viral vector that mediates the stable integration of therapeutic transgenes into the genomes of treated cells and provides sustained expression over a long period of time. Two vectors, the transfer vector pSB-ASNase and the Sleeping Beauty vector SB100, were co-delivered by the PEI-absorbed MSNs into the human lung adenocarcinoma cells. The intracellular asparaginase expression led to the cell cytotoxicity for PC9 and A549 cells. In

addition, the combination of the chemotherapy and the asparaginase gene therapy enhanced the cell cytotoxicity of PC9 and A549 cells. The cisplatin treatment alone resulted in 48 % cell death of PC9, while co-treatment of the cisplatin and MPT increased the death rate to 69 %. Similarly, the doxorubicin treatment alone caused only 22 % of A549 cell death, while the doxorubicin and MPT co-treatment increased the cell death to 63 % (59).

Gene loading and transfection efficiency were increased by surface modification of LPMSNs with positively charged functional groups and genes were protected against enzymatic destruction. Zhan et.al. (2017), prepared hollow MSNs with large pore size (~10 nm) and functionalized with less toxic 1.8 kD PEI. The maximum loading capacity of green fluorescent protein labeled DNA (GFP-DNA) in PEI-HMSNs was found to be 37.98 mg/g indicating that both hollow and large pores contributed to the increase in DNA adsorption. PEI-HMSNs doubled transfection of loaded GFP-DNA plasmid compared to 25 kD PEI confirmed by confocal microscopy (5). Wu et.al. (2015) synthesized mesoporous organosilica nanoparticles (MONs) with micelle/precursor co-templating assembly strategy. Synthesized MONs possessed large nanopores (6.2 nm) and ultrasmall particle sizes (50.75 nm), a large surface area and a high pore volume. In addition, the unique large mesopores and ultrasmall particle sizes of the MONs have been successfully used for for high-throughput intranuclear gene transfer after the stepwise surface conjugations with PEI and TAT pDNA. The loading amount of TAT pDNA was found to be 66.67 μg / mg and two times higher than MSN (33.3 μg / mg). The nuclear-targeting gene-delivery nanoplatform TAT pDNA loaded MONs improved protection for loaded genes, and enhanced transfection efficiencies of plasmids and was found superior to traditional MSNs of small pore sizes (32). In another study, Gao et.al. (2009) reported LPMSNs with 150 nm in size and uniform pores with the large pore entrance size (17.2 nm) and cavity diameter (20.5 nm) by a low temperature (10 °C) synthetic method in the presence of a dual surfactant system. Pluronic F127 used as supramolecular template and co-assembled with hydrolyzed silica species to develop a partially ordered mesophase with face-centered cubic symmetry, a fluorocarbon surfactant with high surface activity (FC-4) surrounded the silica particles through interactions and limited their growth. Furthermore, functionalization of these LPMSNs with aminopropyl groups allowed adsorption of *p*DNA and protected it from enzymatic cleavage (30).

### 4.2.2. Aptamers for targeted delivery of MSNs

Aptamers are synthetic single-stranded oligonucleotides and have a three-dimensional structure that specifically recognizes and binds to target molecules with high affinity. They are desirable candidates for systemic administration and treatment because of their excellent molecular recognition capability, high specificity to target molecules and lower immunogenicity compared to peptides and antibodies (45, 60). Nejabat et.al. (2018), fabricated nucleolin targeted hybrid nanostructure based on hollow MSNs. The surface of doxorubicin-encapsulated hollow MSNs was coated with acetylated carboxymethyl cellulose and then covalently conjugated to the AS1411 aptamer for targeted delivery to nucleolin overexpressed cancerous cells. The size and shell thickness of surface modified hollow MSNs were measured as 150 nm and 30 nm, respectively. AS1411 aptamer showed significant enhancement in cellular uptake and cytotoxicity to MCF-7 and C26 cells *in vitro* compared to non-targeted doxorubicin nanoparticles and free doxorubicin, and specifically targeted nucleolin overexpressing MCF-7 and C26 cells. Furthermore, the *in vivo* tumor inhibitory effect of AS1411 aptamer conjugated formulation also confirmed the efficiency in inhibiting tumor growth and improving the survival rate in comparison with non-targeted and free doxorubicin-treated mice (60). Zahiri et.al. (2019) synthesized doxorubicin-loaded dextran-capped MSNs and attached an RNA aptamer against a cancer stem cell marker CD133 covalently to the carboxyl groups of dextran (Figure 9). The *in vitro* evaluation of cellular uptake and cytotoxicity demonstrated that the produced nanosystem specifically targets colorectal cancer cells (HT29) (45).

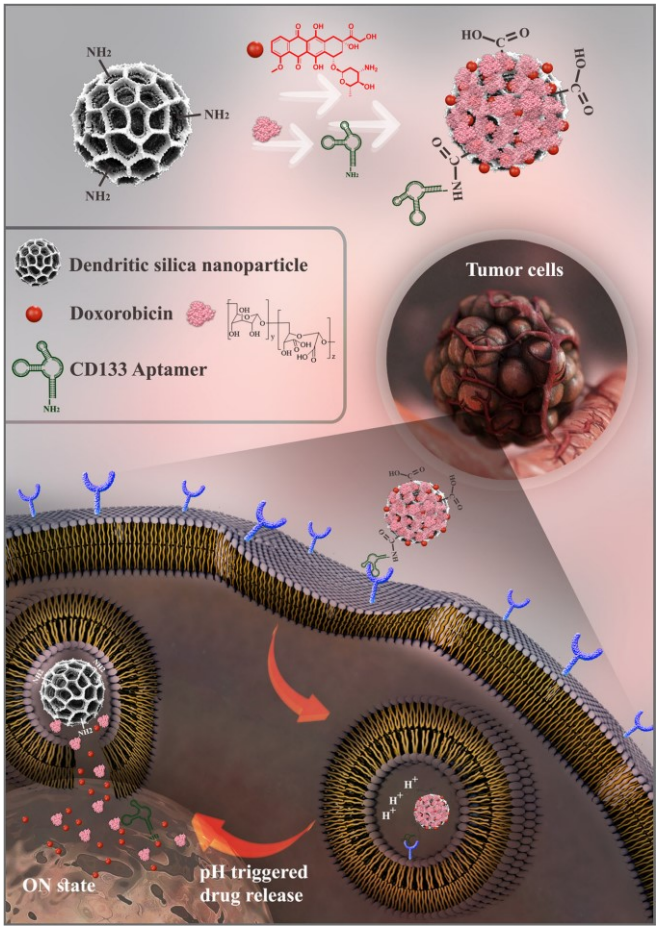


**Figure 9.** Conjugation of CD133-RNA aptamer to the surface of MSNs and specific transportation of encapsulated anticancer drug to CD133 overexpressing cancer cells. Reproduced from Zahiri et.al. (45)

Multifunctional MSNs can combine different materials on a functionalized platform. Since the targeting parts can be easily attached to the MSN surface, intelligent designs can be made. Shen et.al. (2019) fabricated a HApt aptamer-functionalized pH-sensitive β-CD-capped doxorubicin-loaded MSNs (MSN-BM/CD-HApt@DOX) with 218.2 nm in size for targeted delivery and selective targeting of HER2-positive breast cancer. MSN-functionalized with 1-methyl-1H-benzimidazole was used to load and obtain pH stimuli responsive release of the doxorubicin. β-CD exhibited stable hydrophobic interactions with 1-methyl-1H-benzimidazole at physiological pH (7.4), thus introduced as a gatekeeper for encapsulated doxorubicin. HApt was a selective HER2-targeting moiety and biotherapeutic agent and the β-CD-SH was then functionalized with HApt-SH by disulfide bonding. MSN-BM/CD-HApt@DOX underwent HER2-mediated endocytosis and was found to be more cytotoxic to HER2-positive SKBR3 cells than HER2-negative MCF7 cells. MSN-BM/CD-HApt@DOX also exhibited better uptake and stronger growth inhibition in SKBR3 cells than the control MSN-BM/CDNCApt@DOX functionalized with a scrambled nucleotide sequence on CD. Overall, intracellular delivery of doxorubicin and biotherapeutic agent HApt resulted in synergistic cytotoxic effects in HER2-positive cancer cells compared to doxorubicin or HApt alone (46).

**4.2.3. siRNA Delivery**

By inhibiting the expression of targeted genes, small interfering RNAs (siRNAs) are considered as promising therapeutics for the treatment of cancer and genetic disorders. However, the use of siRNA as a therapeutic agent is restricted by its poor cellular uptake and short half-life (61). MSNs have received increasing attention to overcome degradation of siRNA by RNases and to improve intracellular uptake delivery. Hartono et.al. (2012) synthesized LPMSNs less than 200 nm in size and functionalized with PLL consisting of cage-like pores organized in a cubic mesostructure. LP-MSNs were synthesized by a combination of a dual surfactant system, that is, a combination of triblock copolymer (F127) acting as the cubic pore structure directing agent, and a fluorocarbon surfactant (FC-4) to control particle growth. It is noted that the usage of low temperature increases the penetration of the swelling agent TMB into the hydrophobic core of micelles during synthesis, which ultimately results in an extra enlargement of the pore size. The cavity size of LPMSNs was obtained as 27.9 nm, with an entrance size of 13.4 nm. A significant increase of the nanoparticle binding capacity for oligo-DNAs (57 μg/mg) was observed with particle modification by PLL and functionalized nanoparticles showed a strong ability to deliver oligo DNA-Cy3 to Hela cells. Consequently, PLL-functionalized nanoparticles exhibited a strong ability to deliver oligo DNA-Cy3 (a model for siRNA) to Hela cells. The system has also been tested to deliver functional siRNAs against minibrain-related kinase (Mirk) and polo-like kinase 1 (PLK1) in osteosarcoma cancer (KHOS) cells and the cellular viability of osteosarcoma cancer cells was significantly reduced (29).

Recent research has shown that MSN-based gene therapy can be combined with chemotherapy to overcome drug resistance and explore potential therapeutic benefits for the treatment of many complex diseases. Zhang et al. (2019) developed a hybrid MSNs using a layer-by-layer assembly method. Hybrid MSNs were coated with hyaluronic acid (HA), and both disulfide bonds and HA coating of hybrid MSNs facilitated controlled drug release in the tumor microenvironment. Hybrid MSN-HA nanoparticles with negative surface charge were grafted with PEI to increase cellular uptake and gene loading efficiency. *In vitro* release studies indicated that hybrid MSN / HA / PEI can prevent doxorubicin leakage before reaching tumor tissues and is sensitive to intracellular stimuli of hyaluronidase and GSH. Furthermore, the PEI-grafted nanovector showed high siBcl-2 binding efficacy and effectively protected siBcl-2 against enzymatic degradation. Additionally, siBcl-2 and doxorubicin co-loaded hybrid MSNs exhibited the greater growth inhibition against MCF-7 cells compared to single doxorubicin or siBcl-2 showing the synergistic treatment effect of gene and chemical drug on breast cancer (7). Wang et.al. (2018) developed the MSN formulation containing MDR1-siRNA to block MDR1 expression, as well as being able to transport doxorubicin to cancer cells without the effect of multidrug resistance. They modified the surface of MSNs with cationic polymer PEI to obtain positive charge on the surface that would enable them to carry MDR1-siRNA and doxorubicin. Transfection efficacy experiments have shown that modified MSNs are efficiently transfected into doxorubicin resistant (KBV) cells of human oral squamous carcinoma *in vitro*. KBV cells transfected with MSNs were able to effectively reduce gene expression of MDR1 (~ 70% increase after 72 hours of treatment) and induce apoptosis of KBV cells *in vitro* (24.27% after 48 hours of treatment). MSNs dramatically reduced tumor size (81.64% reduction after 28 days post-treatment) and significantly slowed tumor growth rate compared to the *in vivo* control group (62). Wu et.al. (2016) used a selective bond breakage strategy based on the difference in stability for the fabrication of large pore (24nm) HMONs. The basis of this strategy was found to be the expansion of the pore size in the shell as a result of the selective degradation of the weak Si-C bonds due to the difference in chemical bond stability within the framework where the Si-C bond was significantly weaker than the Si-O bond. Subsequently, these mesopores formed larger pores by continuously fusing or merging with each other with the breakage of more Si-C bonds by increasing the hydrothermal temperature (160 °C). A redox-responsive gene release was provided by functionalization with poly (β-amino esters) via a disulfide linker. These functionalized nanocarriers were further used to co-deliver P-gp modulator siRNA (high RNA-loading up to 200 μg/mg) and doxorubicin to reverse the MDR of breast cancer cells. The P-gp expression on MCF-7/ADR membrane was remarkably

downregulated by the developed formulation. The introduction of siRNA significantly increased the doxorubicin concentration in MCF-7/ADR cancer cells, further confirmed by cell apoptosis and cell-cycle change analyzes. Antitumor effect was evaluated in mice bearing MCF-7/ADR tumor xenograft. The tumor volume of the free doxorubicin-treated group was 45.12% of the control group at the end of experiments. Comparatively, the doxorubicin loaded functionalized HMONs group exhibited improved tumor growth inhibitory effect, resulting in a 72.2% reduction in tumor volume. In the functionalized HMONs group where siRNA and doxorubicin were loaded together, the highest antitumor activity was obtained, with a tumor volume only 7.61% of the control group (18).

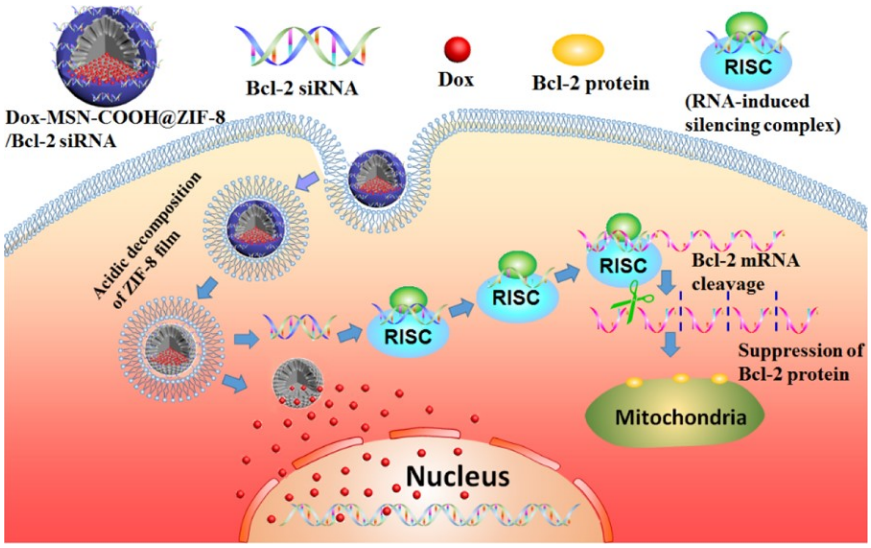


**Figure 10.** Schematic view of a pH sensitive drug delivery system for effective delivery of siRNAs and chemotherapeutics. Reproduced from Pan et.al. (63)

Pan et.al. (2018) synthesized an ultra-thin ZIF-8 film for pore blockage on the MSN surface and fabricated a pH-responsive drug delivery system below 100 nm for efficient delivering siRNAs and therapeutic drugs (Figure 10). The dual delivery of siRNAs and drugs using the ZIF-8 coated MSNs was demonstrated by electrostatic adsorption of Bcl-2 siRNA (98.11%) at the positively charged ZIF-8 film and loading of doxorubicin (59.73 %) into the pores. It is noted that the ZIF-8 film can convert the charge of MSN-COOH from negative to positive for efficient loading of siRNA through electrostatic interactions and protect siRNA from nuclease degradation. The pH-sensitivity of ZIF-8 coated MSNs was confirmed by release studies and TEM. In addition, the ZIF-8 film was reported to dissociate in the acidic endo-lysosome and induce the intracellular release of siRNA and doxorubicin, leading to a significantly enhanced chemotherapeutic efficacy for multidrug-resistant cancer cells including MCF-7/ADR and SKOV-3/ADR (63).

#### 4.2.4. MicroRNA Delivery

MicroRNAs (miRNAs) are a class of small endogenous noncoding RNAs of 18–25 nucleotides in length that functions in RNA silencing and gene expression at the post-transcriptional level. Aberrant expressions of miRNAs have been shown to be associated with tumor onset, progression, and metastasis. Unlike siRNAs with one specific target mRNA, miRNAs can achieve gene-silencing effect by regulating multiple mRNAs, making them effective tools for the treatment of complex multigenic diseases such as cancers. Restoring miRNA function by mimicking miRNA and inhibiting the function of a miRNA with antisense miRNA oligonucleotides (anti-miRs) are the two main strategies of modulating miRNA activity (64). Li et.al. (2018) reported MSNs loaded with anti-miR-155 and modified with polydopamine and AS1411 aptamer

(modified-MSNs) for the targeted treatment of colorectal cancer. Modified-MSNs significantly inhibited the expression of miR-155 and NF-κB (P65) in SW480 cells. Due to the high selectivity, modified-MSNs effectively inhibited tumor growth in SW480 tumor xenograft nude mice compared to the saline control group. The developed modified-MSN formulation was also examined to overcome 5-FU resistance occurring in ~ 90% of patients with colorectal cancer. Combined treatment of free 5-FU and modified-MSNs exhibited higher cytotoxicity on SW480 and SW480/ADR cells, indicating that modified-MSNs successfully increased the sensitivity of SW480 cells to 5-FU. The researchers also evaluated combined antitumor therapy in nude mice with SW480 tumor xenograft. Antitumor therapy of free 5-FU and modified-MSNs could inhibit tumor growth more effectively than free 5-FU (64).

The surface of MSNs is generally functionalized with positive groups to increase the loading of microRNAs and then coated with polymers to increase miRNA stability. In the study of Hu et.al. (2019), anti-miR21 and resveratrol-loaded HA conjugated MSNs with 155 nm hydrodynamic size were developed to enhance therapeutic efficacy in gastric carcinoma. They modified the MSN surface with PEI to load anti-miR21. Since the presence of a protective coating is believed to increase the stability of charged anti-miR21 and can target cancer tissues, the surface was conjugated with HA, which specifically targets receptors in the tumor and potentially enhances cellular internalization. Confocal laser-scanning microscopy and flow cytometry analysis confirmed higher cellular internalization of HA conjugated MSNs. *In vitro* cytotoxicity and apoptosis assays confirmed the superior anticancer effect of the functionalized formulation and synergistic effects of anti-miR21 and resveratrol in gastric cancer cells with apoptosis and cell necrosis mechanisms. A three-fold higher tumor regression effect compared to treatment with free resveratrol and a double tumor regression effect compared to MSNs without HA conjugation were achieved with HA conjugated MSNs (65). Yang et.al. (2019) designed oxaliplatin and miRNA-204-5p loaded PEI-based MSNs with surface conjugated with HA. In addition to the tumor suppressing effect of MiR-204-5p, the anticancer effect of oxaliplatin was aimed to increase synergistically. The oxaliplatin loaded in the pores of the MSN and presence of PEI allowed the loading of miRNA. The final particle size was 138.4 nm with a narrow size distribution. Presence of surface bound HA promoted the selective targeting of its native ligand, CD44 receptors on the colon cancer cells. The target specificity of functionalized formulation was examined in HT-29 cells and improved cellular internalization was observed compared to that of untargeted nanoparticles. Oxaliplatin and miRNA-204-5p loaded PEI-based MSNs with surface conjugated with HA exhibited a higher cell cytotoxicity than the other formulations, indicating that internalization by CD44 receptor-mediated endocytosis was operative. Furthermore, this formulation caused a marked inhibition of tumor growth (66). Wang et.al. (2018) fabricated doxorubicin-loaded MSNs, conjugated miR-31 onto it and coated with PEI/HA. The doxorubicin and miR-31 loading were found to be 6.35 μg/mg and 8.6 nmol/mg, respectively, and drug release was triggered by acidic tumor environment. Co-delivery of miR-31 with doxorubicin within this formulation inhibited the growth of HeLa cells more efficiently than administration of miR-31 or doxorubicin alone (67).

### 5. MSNs for Cancer Immunotherapy

Cancer immunotherapy is currently one of the most promising strategies for cancer treatment. It stimulates the immune system to increase the effectiveness of cancer therapy. Consequently, both tumor recurrence and metastasis can be prevented. Recent studies have focused on the use of mesoporous silica-based adjuvants due to their excellent properties such as large surface areas, adjustable pore size, various morphology, easy adjustment of surface properties, and good biocompatibility. However, there are some limitations in the use of MSN based adjuvants for antitumor immunity. For example, when preparing MSNs with large mesopores to load antigens of larger molecular structure, the particle size also increases and may enter the micron size range. A comparison of antigen- loaded particles of both nanoscaled and micron

sizes (17 μm, 7 μm, 1 μm, and 300 nm diameter) have shown that the smaller-sized particles were more readily taken up by bone-marrow derived dendritic cells, and consequently also more efficient at stimulating antigen-specific effector immune responses *in vivo* (68). Subunit vaccines aiming at induction of cellular (type I) immunity (e.g. cancer vaccines) should thus benefit from encapsulating the antigen in nanoparticles, which consistently outperform microparticles at inducing cytotoxic T cells (69). In the study of Mathaes et.al. (2015) the nanoparticle adjuvant vaccine delivery vehicles displayed a stronger DC activation than the corresponding microparticle counterparts(70). Furthermore, their therapeutic efficacy as an immunoadjuvant is not satisfactory. Therefore, there is still a need to develop a useful and multifunctional MSN adjuvant to overcome obstacles (71).

Recent studies showed that mesoporous silica materials having different particle size, pore structure and surface functionality can modulate T cell activation and proinflammatory cytokine production. Xie et.al. (2017) developed a monodisperse and stable large pore hollow MSN formulation for administration of two melanoma-derived antigenic peptides, HGP100 and TRP2, with different hydrophobicities. The loading efficiencies of the peptides were found as 88% and 20.6%, respectively, by adsorption of the hydrophilic HGP100 peptide after the modification of the hollow core of MSNs with $NH_2$ and hydrophobic TRP2 peptide after COOH modification in porous channels. Hollow MSNs loaded with HGP100 and TRP2 were further encapsulated with liposomes containing the monophosphoryl lipid A (MPLA) adjuvant to improve the stability and biocompatibility of hollow MSNs. This strategy also prevented the leakage of loaded peptides through lipid coating and enhanced antitumor immune responses with the aid of MPLA. The developed hollow MSNs encapsulated with HGP100 (in the hollow core) and TRP2 (in the porous channels) together with MPLA-loaded liposomes (on the outer surface of MSNs) stimulated dendritic cells efficiently, resulting in maturation of dendritic cells and secretion of TNF-α, IFN-γ, IL-12, and IL-4. Active $CD^{8+}$ and $CD^{4+}$ T lymphocytes which secreted IFN-γ in local lymph nodes were also significantly increased *in vivo*. In addition, this formulation led to the inhibition of tumor growth in both B16-F10 prophylactic and lung metastasis models and the delivery system was thought to have great potential for both preventive and therapeutic cancer vaccination (31). Lee et.al. (2019) reported a click reaction-assisted immune cell targeting (CRAIT) strategy that uses inflammatory $CD11b^+$ cells as active carriers to deliver doxorubicin-loaded MSNs to the less vascularized regions of the tumor. For rapid and catalyst-free reaction *in vivo*, they used Tetrazine/ Trans-cyclooctene (TCO) cycloaddition to selectively target doxorubicin-loaded MSNs to $CD11b^+$ cells in blood circulation and tumor microenvironment. Primary administration of TCO-modified $CD11b^+$ antibodies allowed Tz-functionalized MSNs (MSNs-Tz) to be subsequently conjugated onto $CD11b^+$ cells. Real-time intravital imaging of 4T1 tumor-bearing mice showed that $CD11b^+$ cells tagged with MSNs-Tz are highly mobile, crawling and rolling in tumor vasculatures. $CD11b^+$ cell-mediated delivery showed more uniform distribution and deeper tumor penetration of MSNs-Tz than a conventional passive targeting strategy. In the avascular regions of the tumor, MSNs-Tz delivered by the CRAIT strategy showed two times more accumulation than the nanoparticles transported by the EPR effect. Furthermore, doxorubicin delivery rapidly reduced the tumor burden in an aggressive 4T1 breast cancer model without systemic toxicities (72).

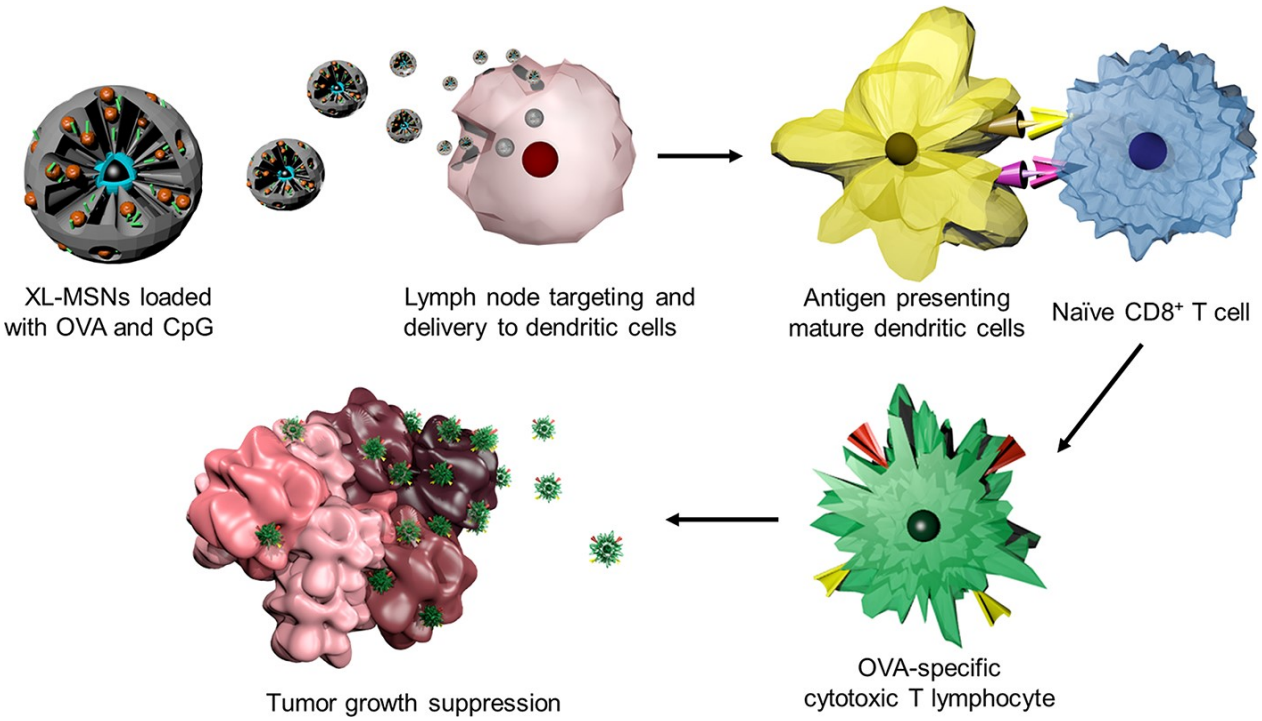


**Figure 11.** Schematic illustration of the overall vaccination process using XL-MSNs loaded with antigen and TLR9 agonist for suppressing tumor growth. Reproduced from Cha et.al. (22)

Ding et al. (2018) produced large-pore mesoporous-silica-coated upconversion nanoparticles (UCMSs) below 100 nm and evaluated its use as an immunoadjuvant. Merocyanine 540 (MC540) as photosensitizer, chicken OVA as model antigen, and CT26 tumor cell fragment (TF) as tumor antigen were loaded to UCMSs and successfully used in colon cancer tumor-bearing BALB / c mice for in vivo vaccine delivery. The prepared MC540 and OVA loaded UCMSs showed the best synergistic immunopotentiation effect under near infrared irradiation at 980 nm. MC540 and TF loaded UCMSs nanovaccine was able to inhibit tumor growth more effectively compared to PDT or immunological therapy alone (73). In another study, Cha et.al. (2018) demonstrated the use of amine-modified XL-MSNs as a cancer vaccine through the delivery of OVA (a model antigenic protein) and CpG oligonucleotide (toll-like receptor 9 (TLR9) agonist). After culture of bone marrow-derived dendritic cells (BMDCs) with antigen and TLR9 agonist-loaded XL-MSNs, the antigen protein and TLR9 agonist was successfully taken up to the cytosol. This led to an increased maturation and antigen presentation of the DCs and increased secretion of proinflammatory cytokines. In the in vivo study, effective targeting to lymph nodes, stimulation of adapted immune responses including antigen-specific cytotoxic T cells, suppression of tumor growth after vaccination, and prevention of tumor growth after substantial vaccination of cancer cells into vaccinated mice due to a significant generation memory T cells were observed (Figure 11) (22). These results showed that MSNs for cancer immunotherapy increase the efficacy and clinical potential of immunotherapy as immunoadjuvant.

## 6. Conclusions and Future Perspectives

The development of various syntheses for LPMSNs have enabled these to be successfully used as delivery vehicles for biomacromolecules. The ceramic silica framework provides efficient protection from the outside environment, providing shelter and stability to the fragile and sensitive biomolecules. The robust inorganic structure further provides ample opportunities for the design of stimuli-responsive drug delivery

systems, especially via the gatekeeping approach. Tuning of the surface chemistry of the carrier can ensure maximized affinity between biomolecular cargo and carrier upon loading. Consequently, numerous examples have been showcased for *in vitro* and *in vivo* delivery of biomacromolecules with the aid of (LP)MSNs as delivery systems.

Recently, there have been many studies aimed at increasing the pore size in order to load higher amounts of biomacromolecules into MSNs. However, expanding the pore size of MSNs for loading biomacromolecules also causes an increase in the MSN size, which hampers the uptake of the final carrier system by cells. Therefore, it is important to consider the pore size and particle size in parallel. In addition, pore sizes slightly larger than the biomacromolecular size are useful for not limiting the diffusion of the biomolecules to the active sites of mesoporous channels, increasing the amount of loading and enhancing immobilization.

The ability of MSNs to carry multiple bioactive molecules together holds great potential particularly in cancer therapy, to produce a synergistic effect to enhance therapeutic efficacy. Co-delivery of chemotherapeutic agents and biomolecules by MSNs with targeting function can increase the cancer cell accumulation and create synergisms in cancer treatment. Despite the proven efficacy of MSNs in numerous preclinical studies, as with any promising nanopharmaceutical, more efforts are needed for their clinical translation.

**References**


1. Benezra M, Penate-Medina O, Zanzonico PB, Schaer D, Ow H, Burns A, et al. Multimodal silica nanoparticles are effective cancer-targeted probes in a model of human melanoma. The Journal of clinical investigation. 2011;121(7):2768-80.
2. Chen F, Goel S, Shi S, Barnhart TE, Lan X, Cai W. General synthesis of silica-based yolk/shell hybrid nanomaterials and in vivo tumor vasculature targeting. Nano Res. 2018;11(9):4890-904.
3. Choi YH, Han HK. Nanomedicines: current status and future perspectives in aspect of drug delivery and pharmacokinetics. Journal of pharmaceutical investigation. 2018;48(1):43-60.
4. Huang M, Liu L, Wang S, Zhu H, Wu D, Yu Z, et al. Dendritic Mesoporous Silica Nanospheres Synthesized by a Novel Dual-Templating Micelle System for the Preparation of Functional Nanomaterials. Langmuir. 2017;33(2):519-26.
5. Zhan Z, Zhang X, Huang J, Huang Y, Huang Z, Pan X, et al. Improved Gene Transfer with Functionalized Hollow Mesoporous Silica Nanoparticles of Reduced Cytotoxicity. Materials (Basel). 2017;10(7).
6. Xu W, Ge P, Niu B, Zhang X, Liu J, Xie J. Macroporous silica nanoparticles for delivering Bcl2-function converting peptide to treat multidrug resistant-cancer cells. Journal of colloid and interface science. 2018;527:141-50.
7. Zhang B, Liu Q, Liu M, Shi P, Zhu L, Zhang L, et al. Biodegradable hybrid mesoporous silica nanoparticles for gene/chemo-synergetic therapy of breast cancer. J Biomater Appl. 2019;33(10):1382-93.
8. Chen C, Tang W, Jiang D, Yang G, Wang X, Zhou L, et al. Hyaluronic acid conjugated polydopamine functionalized mesoporous silica nanoparticles for synergistic targeted chemo-photothermal therapy. Nanoscale. 2019;11(22):11012-24.
9. Yu L, Chen Y, Lin H, Gao S, Chen H, Shi J. Magnesium-Engineered Silica Framework for pH-Accelerated Biodegradation and DNAzyme-Triggered Chemotherapy. Small. 2018;14(35):e1800708.

10. Kao K-C, Lin T-S, Mou C-Y. Enhanced Activity and Stability of Lysozyme by Immobilization in the Matching Nanochannels of Mesoporous Silica Nanoparticles. The Journal of Physical Chemistry C. 2014;118(13):6734-43.
11. Niu D, Liu Z, Li Y, Luo X, Zhang J, Gong J, et al. Monodispersed and ordered large-pore mesoporous silica nanospheres with tunable pore structure for magnetic functionalization and gene delivery. Adv Mater. 2014;26(29):4947-53.
12. Saikia D, Deka JR, Wu CE, Yang YC, Kao HM. pH responsive selective protein adsorption by carboxylic acid functionalized large pore mesoporous silica nanoparticles SBA-1. Mater Sci Eng C Mater Biol Appl. 2019;94:344-56.
13. Siefker J, Karande P, Coppens M-O. Packaging biological cargoes in mesoporous materials: opportunities for drug delivery. Expert opinion on drug delivery. 2014;11(11):1781-93.
14. Kruk M. Access to ultralarge-pore ordered mesoporous materials through selection of surfactant/swelling-agent micellar templates. Acc Chem Res. 2012;45(10):1678-87.
15. Bukara K, Schueller L, Rosier J, Martens MA, Daems T, Verheyden L, et al. Ordered mesoporous silica to enhance the bioavailability of poorly water-soluble drugs: Proof of concept in man. European Journal of Pharmaceutics and Biopharmaceutics. 2016;108:220-5.
16. Xiong L, Bi J, Tang Y, Qiao SZ. Magnetic Core-Shell Silica Nanoparticles with Large Radial Mesopores for siRNA Delivery. Small. 2016;12(34):4735-42.
17. Gu J, Huang K, Zhu X, Li Y, Wei J, Zhao W, et al. Sub-150 nm mesoporous silica nanoparticles with tunable pore sizes and well-ordered mesostructure for protein encapsulation. Journal of colloid and interface science. 2013;407:236-42.
18. Wu M, Meng Q, Chen Y, Zhang L, Li M, Cai X, et al. Large Pore-Sized Hollow Mesoporous Organosilica for Redox-Responsive Gene Delivery and Synergistic Cancer Chemotherapy. Adv Mater. 2016;28(10):1963-9.
19. Meka AK, Abbaraju PL, Song H, Xu C, Zhang J, Zhang H, et al. A Vesicle Supra-Assembly Approach to Synthesize Amine-Functionalized Hollow Dendritic Mesoporous Silica Nanospheres for Protein Delivery. Small. 2016;12(37):5169-77.
20. Rahmani S, Budimir J, Sejalon M, Daurat M, Aggad D, Vives E, et al. Large Pore Mesoporous Silica and Organosilica Nanoparticles for Pepstatin A Delivery in Breast Cancer Cells. Molecules. 2019;24(2).
21. Kwon D, Cha BG, Cho Y, Min J, Park EB, Kang SJ, et al. Extra-Large Pore Mesoporous Silica Nanoparticles for Directing in Vivo M2 Macrophage Polarization by Delivering IL-4. Nano letters. 2017;17(5):2747-56.
22. Cha BG, Jeong JH, Kim J. Extra-Large Pore Mesoporous Silica Nanoparticles Enabling Co-Delivery of High Amounts of Protein Antigen and Toll-like Receptor 9 Agonist for Enhanced Cancer Vaccine Efficacy. ACS central science. 2018;4(4):484-92.
23. Zhang J, Li X, Rosenholm JM, Gu HC. Synthesis and characterization of pore size-tunable magnetic mesoporous silica nanoparticles. Journal of colloid and interface science. 2011;361(1):16-24.
24. Hong Y, Yao Y, Zhao H, Sheng Q, Ye M, Yu C, et al. Dendritic Mesoporous Silica Nanoparticles with Abundant Ti(4+) for Phosphopeptide Enrichment from Cancer Cells with 96% Specificity. Analytical chemistry. 2018;90(12):7617-25.
25. Wang Y, Caruso F. Mesoporous Silica Spheres as Supports for Enzyme Immobilization and Encapsulation. Chemistry of Materials. 2005;17(5):953-61.
26. Kalantari M, Yu M, Yang Y, Strounina E, Gu Z, Huang X, et al. Tailoring mesoporous-silica nanoparticles for robust immobilization of lipase and biocatalysis. Nano Research. 2017;10(2):605-17.
27. Yang J, Tu J, Lamers GEM, Olsthoorn RCL, Kros A. Membrane Fusion Mediated Intracellular Delivery of Lipid Bilayer Coated Mesoporous Silica Nanoparticles. Adv Healthc Mater. 2017;6(20).
28. Slowing, II, Trewyn BG, Lin VS. Mesoporous silica nanoparticles for intracellular delivery of membrane-impermeable proteins. J Am Chem Soc. 2007;129(28):8845-9.

29. Hartono SB, Gu W, Kleitz F, Liu J, He L, Middelberg AP, et al. Poly-L-lysine functionalized large pore cubic mesostructured silica nanoparticles as biocompatible carriers for gene delivery. ACS Nano. 2012;6(3):2104-17.
30. Gao F, Botella P, Corma A, Blesa J, Dong L. Monodispersed mesoporous silica nanoparticles with very large pores for enhanced adsorption and release of DNA. The journal of physical chemistry B. 2009;113(6):1796-804.
31. Xie J, Yang C, Liu Q, Li J, Liang R, Shen C, et al. Encapsulation of Hydrophilic and Hydrophobic Peptides into Hollow Mesoporous Silica Nanoparticles for Enhancement of Antitumor Immune Response. Small. 2017;13(40).
32. Wu M, Meng Q, Chen Y, Du Y, Zhang L, Li Y, et al. Large-pore ultrasmall mesoporous organosilica nanoparticles: micelle/precursor co-templating assembly and nuclear-targeted gene delivery. Adv Mater. 2015;27(2):215-22.
33. Hartono SB, Yu M, Gu W, Yang J, Strounina E, Wang X, et al. Synthesis of multi-functional large pore mesoporous silica nanoparticles as gene carriers. Nanotechnology. 2014;25(5):055701.
34. Zheng Q, Lin T, Wu H, Guo L, Ye P, Hao Y, et al. Mussel-inspired polydopamine coated mesoporous silica nanoparticles as pH-sensitive nanocarriers for controlled release. International journal of pharmaceutics. 2014;463(1):22-6.
35. Liu HJ, Xu P. Smart Mesoporous Silica Nanoparticles for Protein Delivery. Nanomaterials (Basel). 2019;9(4).
36. Qiao H, Jia J, Shen H, Zhao S, Chen E, Chen W, et al. Capping Silica Nanoparticles with Tryptophan-Mediated Cucurbit[8]uril Complex for Targeted Intracellular Drug Delivery Triggered by Tumor-Overexpressed IDO1 Enzyme. Adv Healthc Mater. 2019;8(13):e1900174.
37. Li E, Yang Y, Hao G, Yi X, Zhang S, Pan Y, et al. Multifunctional Magnetic Mesoporous Silica Nanoagents for in vivo Enzyme-Responsive Drug Delivery and MR Imaging. Nanotheranostics. 2018;2(3):233-42.
38. Portilho FL, Pinto SR, de Barros A, Helal-Neto E, Dos Santos SN, Bernardes ES, et al. In loco retention effect of magnetic core mesoporous silica nanoparticles doped with trastuzumab as intralesional nanodrug for breast cancer. Artif Cells Nanomed Biotechnol. 2018;46(sup3):S725-S33.
39. Siminzar P, Omidi Y, Golchin A, Aghanejad A, Barar J. Targeted delivery of doxorubicin by magnetic mesoporous silica nanoparticles armed with mucin-1 aptamer. Journal of drug targeting. 2019:1-10.
40. Sakhtianchi R, Darvishi B, Mirzaie Z, Dorkoosh F, Shanehsazzadeh S, Dinarvand R. Pegylated magnetic mesoporous silica nanoparticles decorated with AS1411 Aptamer as a targeting delivery system for cytotoxic agents. Pharm Dev Technol. 2019;24(9):1063-75.
41. Li X, Fan H, Guo T, Bai H, Kwon N, Kim KH, et al. Sequential Protein-Responsive Nanophotosensitizer Complex for Enhancing Tumor-Specific Therapy. ACS Nano. 2019;13(6):6702-10.
42. Er O, Colak SG, Ocakoglu K, Ince M, Bresoli-Obach R, Mora M, et al. Selective Photokilling of Human Pancreatic Cancer Cells Using Cetuximab-Targeted Mesoporous Silica Nanoparticles for Delivery of Zinc Phthalocyanine. Molecules. 2018;23(11).
43. Fang J, Wang Q, Yang G, Xiao X, Li L, Yu T. Albumin-MnO2 gated hollow mesoporous silica nanosystem for modulating tumor hypoxia and synergetic therapy of cervical carcinoma. Colloids and surfaces B, Biointerfaces. 2019;179:250-9.
44. Paris JL, de la Torre P, Cabanas MV, Manzano M, Flores AI, Vallet-Regi M. Suicide-gene transfection of tumor-tropic placental stem cells employing ultrasound-responsive nanoparticles. Acta Biomater. 2019;83:372-8.
45. Zahiri M, Babaei M, Abnous K, Taghdisi SM, Ramezani M, Alibolandi M. Hybrid nanoreservoirs based on dextran-capped dendritic mesoporous silica nanoparticles for CD133-targeted drug delivery. J Cell Physiol. 2019.

46. Shen Y, Li M, Liu T, Liu J, Xie Y, Zhang J, et al. A dual-functional HER2 aptamer-conjugated, pH-activated mesoporous silica nanocarrier-based drug delivery system provides in vitro synergistic cytotoxicity in HER2-positive breast cancer cells. International journal of nanomedicine. 2019;14:4029-44.
47. Liu CM, Chen GB, Chen HH, Zhang JB, Li HZ, Sheng MX, et al. Cancer cell membrane-cloaked mesoporous silica nanoparticles with a pH-sensitive gatekeeper for cancer treatment. Colloids and surfaces B, Biointerfaces. 2019;175:477-86.
48. Kuang Y, Chen H, Chen Z, Wan L, Liu J, Xu Z, et al. Poly(amino acid)/ZnO/mesoporous silica nanoparticle based complex drug delivery system with a charge-reversal property for cancer therapy. Colloids and surfaces B, Biointerfaces. 2019;181:461-9.
49. Yang X, Trinh HM, Agrahari V, Sheng Y, Pal D, Mitra AK. Nanoparticle-Based Topical Ophthalmic Gel Formulation for Sustained Release of Hydrocortisone Butyrate. AAPS PharmSciTech. 2016;17(2):294-306.
50. Shao D, Li M, Wang Z, Zheng X, Lao YH, Chang Z, et al. Bioinspired Diselenide-Bridged Mesoporous Silica Nanoparticles for Dual-Responsive Protein Delivery. Adv Mater. 2018:e1801198.
51. Zhang J, Shen B, Chen L, Chen L, Meng Y, Feng J. A dual-sensitive mesoporous silica nanoparticle based drug carrier for cancer synergetic therapy. Colloids and surfaces B, Biointerfaces. 2019;175:65-72.
52. Jimenez-Falcao S, Joga N, Garcia-Fernandez A, Llopis Lorente A, Torres D, de Luis B, et al. Janus nanocarrier powered by bi-enzymatic cascade system for smart delivery. J Mater Chem B. 2019;7(30):4669-76.
53. Agostini A, Mondragon L, Pascual L, Aznar E, Coll C, Martinez-Manez R, et al. Design of enzyme-mediated controlled release systems based on silica mesoporous supports capped with ester-glycol groups. Langmuir. 2012;28(41):14766-76.
54. Deodhar GV, Adams ML, Trewyn BG. Controlled release and intracellular protein delivery from mesoporous silica nanoparticles. Biotechnol J. 2017;12(1).
55. Xu C, Lei C, Yu C. Mesoporous Silica Nanoparticles for Protein Protection and Delivery. Front Chem. 2019;7:290.
56. Tambe P, Kumar P, Paknikar KM, Gajbhiye V. Decapeptide functionalized targeted mesoporous silica nanoparticles with doxorubicin exhibit enhanced apoptotic effect in breast and prostate cancer cells. International journal of nanomedicine. 2018;13:7669-80.
57. Bhattacharyya S, Wang H, Ducheyne P. Polymer-coated mesoporous silica nanoparticles for the controlled release of macromolecules. Acta Biomater. 2012;8(9):3429-35.
58. Solberg SM, Landry CC. Adsorption of DNA into mesoporous silica. The journal of physical chemistry B. 2006;110(31):15261-8.
59. Chang JH, Mou KY, Mou CY. Sleeping Beauty Transposon-Mediated Asparaginase Gene Delivery by a Nanoparticle Platform. Scientific reports. 2019;9(1):11457.
60. Nejabat M, Mohammadi M, Abnous K, Taghdisi SM, Ramezani M, Alibolandi M. Fabrication of acetylated carboxymethylcellulose coated hollow mesoporous silica hybrid nanoparticles for nucleolin targeted delivery to colon adenocarcinoma. Carbohydrate polymers. 2018;197:157-66.
61. Pinese C, Lin J, Milbreta U, Li M, Wang Y, Leong KW, et al. Sustained delivery of siRNA/mesoporous silica nanoparticle complexes from nanofiber scaffolds for long-term gene silencing. Acta Biomater. 2018;76:164-77.
62. Wang D, Xu X, Zhang K, Sun B, Wang L, Meng L, et al. Codelivery of doxorubicin and MDR1-siRNA by mesoporous silica nanoparticles-polymerpolyethylenimine to improve oral squamous carcinoma treatment. International journal of nanomedicine. 2018;13:187-98.
63. Pan QS, Chen TT, Nie CP, Yi JT, Liu C, Hu YL, et al. In Situ Synthesis of Ultrathin ZIF-8 Film-Coated MSNs for Codelivering Bcl 2 siRNA and Doxorubicin to Enhance Chemotherapeutic Efficacy in Drug-Resistant Cancer Cells. ACS Appl Mater Interfaces. 2018;10(39):33070-7.

64. Li Y, Duo Y, Bi J, Zeng X, Mei L, Bao S, et al. Targeted delivery of anti-miR-155 by functionalized mesoporous silica nanoparticles for colorectal cancer therapy. International journal of nanomedicine. 2018;13:1241-56.
65. Hu Y, Wang Z, Qiu Y, Liu Y, Ding M, Zhang Y. Anti-miRNA21 and resveratrol-loaded polysaccharide-based mesoporous silica nanoparticle for synergistic activity in gastric carcinoma. Journal of drug targeting. 2019:1-9.
66. Yang H, Liu Y, Qiu Y, Ding M, Zhang Y. MiRNA-204-5p and oxaliplatin-loaded silica nanoparticles for enhanced tumor suppression effect in CD44-overexpressed colon adenocarcinoma. International journal of pharmaceutics. 2019;566:585-93.
67. Wang F, Zhang L, Bai X, Cao X, Jiao X, Huang Y, et al. Stimuli-Responsive Nanocarrier for Co-delivery of MiR-31 and Doxorubicin To Suppress High MtEF4 Cancer. ACS Appl Mater Interfaces. 2018;10(26):22767-75.
68. Joshi VB, Geary SM, Salem AK. Biodegradable particles as vaccine delivery systems: size matters. The AAPS journal. 2013;15(1):85-94.
69. Slutter B, Jiskoot W. Sizing the optimal dimensions of a vaccine delivery system: a particulate matter. Expert opinion on drug delivery. 2016;13(2):167-70.
70. Mathaes R, Winter G, Siahaan TJ, Besheer A, Engert J. Influence of particle size, an elongated particle geometry, and adjuvants on dendritic cell activation. European journal of pharmaceutics and biopharmaceutics : official journal of Arbeitsgemeinschaft fur Pharmazeutische Verfahrenstechnik eV. 2015;94:542-9.
71. Ding D, Zhu Q. Recent advances of PLGA micro/nanoparticles for the delivery of biomacromolecular therapeutics. Mater Sci Eng C Mater Biol Appl. 2018;92:1041-60.
72. Lee SH, Park OK, Kim J, Shin K, Pack CG, Kim K, et al. Deep Tumor Penetration of Drug-Loaded Nanoparticles by Click Reaction-Assisted Immune Cell Targeting Strategy. J Am Chem Soc. 2019.
73. Ding B, Shao S, Yu C, Teng B, Wang M, Cheng Z, et al. Large-Pore Mesoporous-Silica-Coated Upconversion Nanoparticles as Multifunctional Immunoadjuvants with Ultrahigh Photosensitizer and Antigen Loading Efficiency for Improved Cancer Photodynamic Immunotherapy. Adv Mater. 2018;30(52):e1802479.